Impact of Nonlinear Distortion in Radio over Fiber Systems with Single-Side Band and Tandem Single-Side Band Subcarrier Modulations

Caiqin Wu

A Thesis

in

The Department

of

Electrical and Computer Engineering

Presented in Partial Fulfillment of the Requirements

for the Degree of Master of Applied Science

at

Concordia University

Montreal, Quebec, Canada

November 2005

Your file Votre référence
ISBN: 0-494-14286-3
Our file Notre référence
ISBN: 0-494-14286-3

Abstract

Impact of Nonlinear Distortion in Radio over Fiber Systems with Single-Side Band and Tandem Single-Side Band Subcarrier Modulations

Caiqin Wu

In radio over fiber (RoF) systems there are two popular optical subcarrier modulations (SCMs) which are single side band (SSB) modulation and tandem single side band (TSSB) modulation. In TSSB modulation one optical carrier carries half of radio frequency (RF) signal tones to lower sideband (LSB) and the reminder to upper sideband (USB); while in SSB modulation all multiple RF signal tones in either LSB or USB.

We analyze the impact of nonlinear distortion considering one wavelength carrying two RF signals. For small modulation depth TSSB and SSB SCMs lead to similar and very small nonlinear distortion. Because harmonic distortions (HDs) and inter-modulation distortion (IMDs) are strongly dependent on modulation depth, TSSB and SSB SCMs lead to different nonlinear distortion if modulation depth is not small, depending on two RF difference. To reduce nonlinear distortion for high modulation depth the two RF difference of 1GHz is preferred for both TSSB and SSB SCMs because some nonlinear distortions are dependent on the difference and sum of the two RFs and transmission fiber. However for the larger RF difference, either small modulation depth or medium modulation depth combined with minimum RF of 6GHz has to be used.

Comparison of TSSB and SSB SCMs in DWDM RoF systems with 12.5GHz channel spacing and two subcarriers uniformly distributed in the optical spectrum shows that better performance is obtained using SSB SCM when small modulation depth is used. On the contrary, TSSB SCM is better than SSB SCM when large modulation depth is used.

Acknowledgements

I thank God for everything.

I would like to express my sincere thanks to Prof. Xiupu Zhang for providing an opportunity to study on a MASc program in Electrical and Computer Engineering. I especially thank Prof. Xiupu Zhang for precious guidance, instructions and advices.

I also thank all people at the Department of Electrical and Computer Engineering for their help.

Finally I thank my husband Yonggang Hong's support all the time.

Caiqin Wu

Table of contents

Acronyms and Abbreviations

RoF	Radio over fiber
SCM	Sub-carrier modulation
DWDM	Dense-wavelength-division-multiplexing
TSSB	Tandem single side band
SSB	Single side band
RF	Radio frequency
MZM	Mach-Zehnder modulator
HD	Harmonic distortion
IMD	Inter-modulation distortion
LSB	Lower sideband
USB	Upper sideband
FDM	Frequency division multiplexing
NSR	Noise to signal ratio
BER	Bit error ratio

Chapter 1 Introduction

Wireless communication, being the most convenient of communication systems, continues to increase in popularity. However, disadvantages of wireless systems include narrow bandwidth and limited frequency. In order to use the same frequency repetitively and efficiently, the pico-cell wireless system is investigated [1][2], since the average cell is typically less than 400 feet in diameter, a large number of the base stations are required for effective signal distribution over a given area. Future wireless networks, must therefore require cost-effective technology for the transmission of radio signals from central stations to base stations. A new technology was proposed to transmit the radio signals through fiber optic systems starting from the central station and heading towards the base stations. This is called radio over fiber (RoF) technology, which has been investigated for mobile and personal communication and may be applied combined with coarse/dense wave length division multiplexing (C/DWDM) [3]-[10].

1.1 Optical subcarrier modulation techniques in radio over fiber systems

In this thesis, radio frequency subcarrier transmitted by optic link is used for the purpose of supplying broadband signals to a large number of base stations. One of the key parts of the optical link is optical subcarrier modulation. We will focus on the investigation of two main optical subcarrier modulations.

In fiber optic system, the standard optical channel space is 200GHz, 100GHz, 50GHz 25GHz and 12.5GHz. In order to use the optical fiber bandwidth efficiently, we consider the optical channel space of 12.5GHz. We also use single side band modulation for eliminating one side subcarriers, which save the bandwidth and thus more subcarrier signals can be transmitted in one optical channel. Furthermore, in order to improve optic spectral efficiency in transmission and reduce chromatic dispersion impact on transmission, new modulation with one optical wavelength carrying two or more subcarrier signals has been proposed [11]-[13]. Two different subcarrier modulations can be used: tandem single side band (TSSB) modulation and single side band (SSB) modulation. In TSSB modulation, one optical carrier contains half of Radio frequency (RF) or frequency division multiplexing (FDM) signal tones allocated to low sideband (LSB) and the reminder to upper sideband (USB); while in SSB modulation one optical carrier can carry multiple RF or FDM signal tones in either LSB or USB, therefore the spectral efficiency of both modulations can be the same.

1.2 Nonlinear distortion caused by optical subcarrier modulations

Since optical fiber transmission system has a good anti-interference ability, interference from related environment or optical devices can be ignored. The main interference is nonlinear distortion because of the optical subcarrier modulation. Both TSSB and SSB modulations can be accomplished by using Mach-Zehnder modulators (MZMs), which theoretically have a squared cosine transfer function in power. In other words, MZMs have nonlinear transfer functions, resulting in nonlinear distortion which consists of harmonic distortions (HDs) and inter-modulation distortions (IMDs). The IMDs can be increased significantly when multiple radio frequency (RF) signals or frequency division multiplexed (FDM) signals are carried by one optical carrier. Such nonlinear distortions would considerably reduce receiver sensitivity and dynamic range [5], [14]-[16]. Intuitively, since the spectral efficiency of both TSSB and SSB modulations can be the same, one might expect that two modulations might have the same nonlinear distortion. However, nonlinear distortions in these two cases haven't so far been carefully investigated.

In these two modulations, nonlinear distortion between the RF signals is different either in single optical channel or in multiple optical channel DWDM transmission system. Even in same modulation for either TSSB or SSB with different optical modulation depth, the nonlinear distortion will be different, considering one optical carrier containing two RF signal tones using an MZM. We analyzed and compared the nonlinear distortions for one optical carrier having both SSB modulation and TSSB modulation. Moreover, interference due to nonlinear distortions in dense WDM systems was analyzed by simulation.

1.3 Organization of this thesis

Chapter 2 provides the theoretical analysis of nonlinear distortion caused by the two optical subcarrier modulations. We derivate the output signals for TSSB and SSB modulations, and study the nonlinear distortion between two RF signals in the same optical channel with different optical fiber length and optical modulation depth. Then we also investigate nonlinear distortion from different optical channels, with different optical modulation depth of 0.1, 1 and 1.7, and also compare the distortion interference between the TSSB and the SSB modulations. Chapter 3 verifies the theoretical analysis in Chapter 2 by using simulations, and also compares nonlinear distortion of TSSB and SSB modulations in DWDM systems. Then, Chapter 4 summarizes the thesis and a conclusion is drawn.

Chapter 2 Theoretical Analysis of Nonlinear Distortion

2.1 SSB modulation in single channel radio over fiber systems with one optical subcarrier

The ideal Mach-Zehnder modulator was used to get optical single sideband modulation, Figure 2.1 shows the schematic structure of Mach-Zehnder interferometer type modulator. RF signal is applied to both electrodes with $\pi/2$ phase delay in one electrode, a DC bias sets the modulator at a quadrature. This means that the DC in one arm is half of the bias voltage and the other arm is put to the ground.

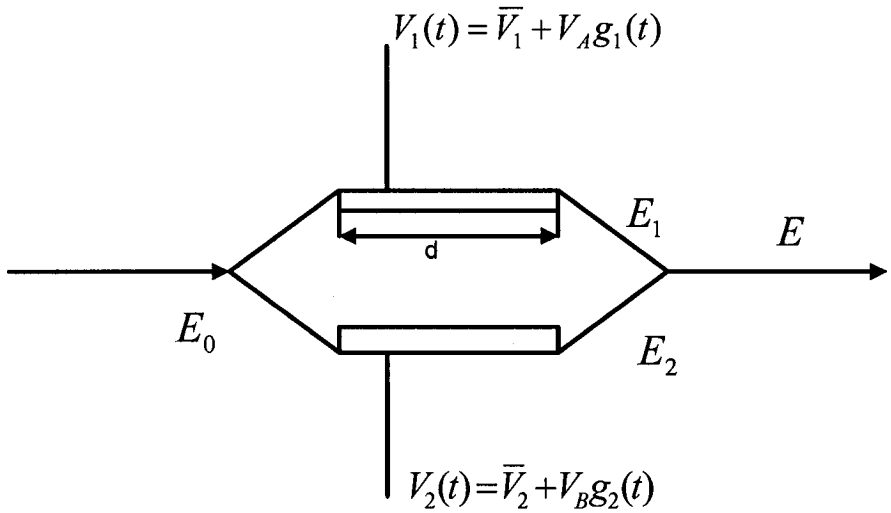

Figure 2.1 The schematic structure of Mach-Zehnder interferometer type modulator.

The electric field for each arm corresponding to Figure 2.1 can be written as

$$E_1 = \frac{1}{2} E_0 \exp(-i\omega t + i\Delta\beta_1 d) \tag{2.1}$$

$$E_2 = \frac{1}{2} E_0 \exp(-i\omega t + i\Delta\beta_2 d) \tag{2.2}$$

The combined electric field is then given by

$$E = E_1 + E_2 = \frac{1}{2} E_0 \exp(-i\omega t)\cos\left[\frac{\Delta\beta_1 - \Delta\beta_2}{2} d\right]\exp\left[i\left(\frac{\Delta\beta_1 + \Delta\beta_2}{2}\right)d\right] \tag{2.3}$$

Where $\Delta\beta_1$ and $\Delta\beta_2$ are the propagation constants in the two waveguide arms respectively, and d is the length of the arm. In addition, we can obtain

$$\Delta\beta_1 d = \pi \frac{V_A g_1(t)}{V_\pi} + \pi \frac{\overline{V}_1}{V_\pi} \tag{2.4}$$

$$\Delta\beta_2 d = \pi \frac{V_B g_2(t)}{V_\pi} + \pi \frac{\overline{V}_2}{V_\pi} \tag{2.5}$$

Where E_0 is the input optical signal, ω is the frequency of the optical signal, V_A and V_B are the constant driving voltages for the two arms, $\overline{V}_1$ and $\overline{V}_2$ are DC bias voltages. $g_1(t)$ and $g_2(t)$ are modulated signals, V_π is the voltage inducing a π phase shift in each arm of the MZM.

Since RF signals at the two electrodes of the MZM modulator must be a Hilbert transform pair, which means that one of two RF signals has to pass through a 90^0 phase shifter and the modulator is DC biased at a quadrature point of the nonlinear electrical to optical transfer curve of the modulator to avoid second-order nonlinear distortions. We set $g_1(t) = V_A \cos\Omega t$, Ω is radio frequency of RF signal,

$g_1(t) = V_A \cos \Omega t$ through a 90^0 phase shifter and the signal is $g_2(t) = V_B \cos\left(\Omega t + \frac{\pi}{2}\right) = -V_B \sin \Omega t$. Let us set $V_A = V_B = V_m$, $\overline{V}_1 = \frac{1}{2} V_\pi$. Then we put $g_1(t) = V_m \cos \Omega t$ and $g_2(t) = -V_m \sin \Omega t$ into equation (2.4) and (2.5), then with equation (2.3), (2.4) and (2.5), we get the modulated optical signal from the MZM modulator

$$E = E_1 + E_2 = \frac{1}{2} E_0 \exp(-i\omega t) \cos\left[\frac{V_m \pi}{2V_\pi} \cos \Omega t + \frac{\pi}{4} - \frac{V_m \pi}{2V_\pi} \sin \Omega t\right] \exp\left[i\left(\frac{V_m \pi}{2V_\pi} \cos \Omega t + \frac{\pi}{4} + \frac{V_m \pi}{2V_\pi} \sin \Omega t\right)\right] \tag{2.6}$$

If we define optical modulation depth $\xi\pi = \frac{V_m}{V_\pi} \pi$, according to the Bessel function, then (2.6) becomes

$$E = \frac{E_0}{\sqrt{2}} \left\{ \sqrt{2} J_0(\xi\pi) \cos\left(\omega t + \frac{\pi}{4}\right) - 2J_1(\xi\pi) \cos(\omega + \Omega)t \right.$$
$$\left. + \sqrt{2} J_2(\xi\pi)(\cos(\omega + 2\Omega)t + \cos(\omega - 2\Omega)t) + 2\cos((\omega - 3\Omega)t) + \ldots \right\} \tag{2.7}$$

After photo detector, the current is given by

$$I = \Re \eta |E_{out}|^2 \approx \frac{\Re \eta |E_0|^2}{2} \left\{ J_0{}^2(\xi\pi) - 2\sqrt{2} J_0(\xi\pi) J_1(\xi\pi) \cos\left(\Omega t - \frac{\pi}{4}\right) \right.$$
$$+ \sqrt{2} J_0(\xi\pi) J_2(\xi\pi) \cos\left(2\Omega t - \frac{\pi}{4}\right)$$
$$\left. - 2\sqrt{2} J_0(\xi\pi) J_3(\xi\pi) \sin\left(3\Omega t + \frac{\pi}{4}\right) + \bullet\bullet\bullet \right\} \tag{2.8}$$

The optical spectra corresponding to (2.7) are shown in Figure 2.2 (a), and the electrical spectra corresponding to (2.8) are shown in Figure 2.2 (b).

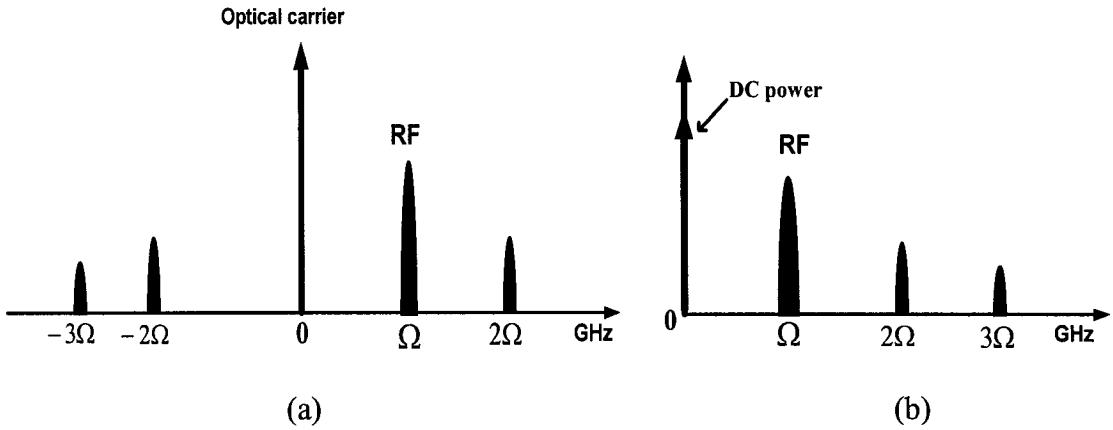

Figure 2.2 (a) the optical and (b) electrical spectra of the single side band modulation.

In the optical spectra diagram in Figure 2.2 (a), there are optical carrier, single side subcarrier RF, and HDs at $\pm 2\Omega$ and -3Ω in frequency. MZM modulator will generate harmonic distortion HDs if one optical wavelength carries one RF subcarrier.

2.2 TSSB modulation in single channel radio over fiber systems

In order to use both upper and lower sidebands of the optical carrier, one optical wavelength will carry two or more different RF subcarriers, half of subcarriers are located in LSB and the reminder in USB. We analyzed one optical carrier containing two RF subcarriers without loss of the generality. Two sets of the data modulated by the microwave carriers are simultaneously applied, with both signals delayed for 90^0 and combined through a 4-port and 90^0 RF hybrid. This means that RF1 signal is combined

with 90^0 delayed RF2 signal, and RF2 signal is combined with 90^0 delayed RF1 signal. Then these two combined signals were injected into two ports of the MZM modulator. The principle diagram of TSSB is shown in Figure 2.3.

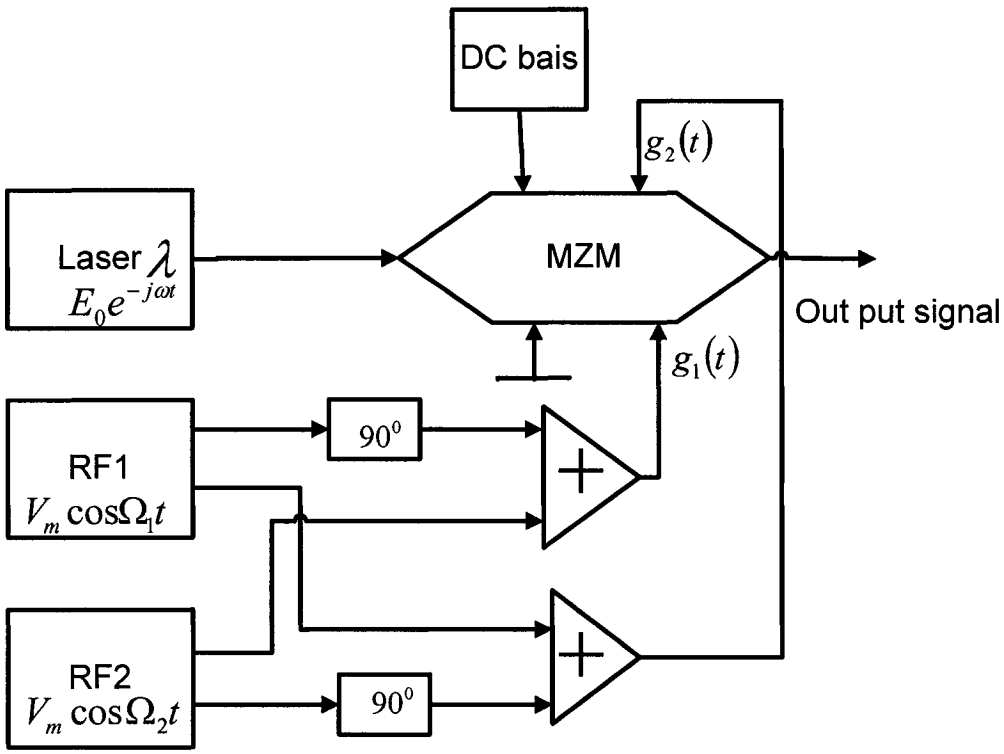

Figure 2.3 The principle diagram of TSSB modulation.

In Figure 2.3, input signals in both ports are the combination of two RF signals. RF1 signal is $V_m \cos\Omega_1 t$ and the RF2 signal is $V_m \cos\Omega_2 t$, and each of the RF signal is separated to two parts and one of the part is 90^0 phase delayed; then they are combined together, i.e.

$$g_1(t) = V_m \cos\Omega_1 t + V_m \cos\left(\Omega_2 t + \frac{\pi}{2}\right) = V_m(\cos\Omega_1 t - \sin\Omega_2 t) \tag{2.9}$$

$$g_2(t) = V_m \cos\Omega_2 t + V_m \cos\left(\Omega_1 t + \frac{\pi}{2}\right) = -V_m(\sin\Omega_1 t - \cos\Omega_2 t) \tag{2.10}$$

Optical carrier signal is $E_{in} = E_0 e^{-j\omega t}$ (2.11)

From the detail derivation given in Appendix, we obtain the output electric field from the MZM modulator as follows:

$$\begin{aligned}
E_{out} = \frac{E_0}{\sqrt{2}}\Bigg\{ & \sqrt{2}J_0^{\,2}(\xi\pi)\cos\left(\omega t + \frac{\pi}{4}\right) - 2J_0(\xi\pi)J_1(\xi\pi)\cos(\omega t + \Omega_1 t) - 2J_0(\xi\pi)J_1(\xi\pi)\sin(\omega t - \Omega_2 t) \\
& + \sqrt{2}J_1^{\,2}(\xi\pi)\sin\left(\omega t + (\Omega_2 - \Omega_1)t - \frac{\pi}{4}\right) - \sqrt{2}J_1^{\,2}(\xi\pi)\sin\left(\omega t - (\Omega_2 - \Omega_1)t - \frac{\pi}{4}\right) \\
& + \sqrt{2}J_1^{\,2}(\xi\pi)\sin\left(\omega t + (\Omega_2 + \Omega_1)t + \frac{\pi}{4}\right) - \sqrt{2}J_1^{\,2}(k)\sin\left(\omega t - (\Omega_1 + \Omega_2)t + \frac{\pi}{4}\right) \\
& - 2J_1(\xi\pi)J_2(\xi\pi)\cos\left(\omega t - (2\Omega_2 + \Omega_1)t\right) + 2J_1(\xi\pi)J_2(\xi\pi)\cos\left(\omega t - (2\Omega_2 - \Omega_1)t\right) \\
& + 2J_1(\xi\pi)J_2(\xi\pi)\sin(\omega t + (2\Omega_1 + \Omega_2)t) + 2J_1(\xi\pi)J_2(\xi\pi)\sin(\omega t + (2\Omega_1 - \Omega_2)t) \\
& + \sqrt{2}J_0(\xi\pi)J_2(\xi\pi)\cos\left(\omega t + 2\Omega_1 t - \frac{\pi}{4}\right) + \sqrt{2}J_0(\xi\pi)J_2(\xi\pi)\cos\left(\omega t - 2\Omega_1 t - \frac{\pi}{4}\right) \\
& - \sqrt{2}J_0(\xi\pi)J_2(\xi\pi)\cos\left(\omega t + 2\Omega_2 t - \frac{\pi}{4}\right) - \sqrt{2}J_0(\xi\pi)J_2(\xi\pi)\cos\left(\omega t - 2\Omega_2 t - \frac{\pi}{4}\right) \\
& - 2J_2^2(\xi\pi)\cos\left(\omega t + 2(\Omega_2 - \Omega_1)t + \frac{\pi}{4}\right) - 2J_2^2(\xi\pi)\cos\left(\omega t - 2(\Omega_2 - \Omega_1)t + \frac{\pi}{4}\right) \\
& - 2J_1(\xi\pi)J_3(\xi\pi)\sin\left(\omega t + (3\Omega_1 - \Omega_2)t - \frac{\pi}{4}\right) - 2J_1(\xi\pi)J_3(\xi\pi)\sin\left(\omega t - (3\Omega_1 - \Omega_2)t - \frac{\pi}{4}\right) \\
& + 2J_0(\xi\pi)J_3(\xi\pi)\cos(\omega t - 3\Omega_1 t) + \cdots\Bigg\}
\end{aligned} \tag{2.12}$$

where $J_k(\ )$ is the Bessel function of first kind, k=0, 1, 2, 3 …, and $\xi = V_m/V_\pi$ is

optical modulation index, V_m - RF modulation voltage at two arms, and V_π - the voltage inducing a π phase shift in each arm of the MZM. In (2.12), the first term represents the optical carrier, the second and third terms are the USB subcarriers and LSB subcarriers which carry different RF data, and all others are either IMDs or HDs. The IMDs occur at $-(\Omega_2-\Omega_1)$, $(\Omega_2-\Omega_1)$, $-(2\Omega_2-\Omega_1)$, $(2\Omega_1-\Omega_2)$, $(\Omega_1+\Omega_2)$, $-(\Omega_1+\Omega_2)$, $-(2\Omega_2+\Omega_1)$, $(2\Omega_1+\Omega_2)$, $2(\Omega_2-\Omega_1)$, $-2(\Omega_2-\Omega_1)$, $(3\Omega_2-\Omega_1)$ and $-(3\Omega_2-\Omega_1)$ etc; and the HDs occur at $2\Omega_1$, $-2\Omega_1$, $2\Omega_2$, $-2\Omega_2$, $-3\Omega_1$, and $3\Omega_2$ etc. In order for better knowing HD and IMD frequency locations relative to the two optical signal subcarriers, let us consider a case of $\Omega_1=4$GHz, and $\Omega_2=7$GHz without loss of the generality. Thus, we obtain $\pm(\Omega_2-\Omega_1)=\pm3$ GHz, $\pm2(\Omega_2-\Omega_1)=\pm6$ GHz, $-(2\Omega_2-\Omega_1)=$ -10 GHz, $(2\Omega_1-\Omega_2)$=1 GHz, $\pm(\Omega_1+\Omega_2)=\pm11$ GHz, $\pm2\Omega_1=\pm8$ GHz, and $\pm2\Omega_2=\pm14$ GHz etc. If optical channel spacing of 12.5 GHz in DWDM is considered, nonlinear distortions with frequencies of beyond channel pass-band are supposed to be suppressed by optical filtering. Therefore, nonlinear distortion may be introduced from IMDs at $-(2\Omega_2-\Omega_1)$, $\pm2(\Omega_2-\Omega_1)$, $\pm(\Omega_2-\Omega_1)$ and $(2\Omega_1-\Omega_2)$, and from HD at $\pm2\Omega_1$ for the above case. Note that when $\Omega_1=\Omega_2$, $-(2\Omega_2-\Omega_1)=-\Omega_1=-\Omega_2$, $(2\Omega_1-\Omega_2)=\Omega_1=\Omega_2$, these two IMDs are overlapped with the two RF subcarriers, and thus the worst nonlinear distortion occurs. However, some IMDs and HDs will not be suppressed by optical filtering because they are close to the two RF subcarriers and within the pass-band of DWDM multiplexer. If we only consider the IMDs and HDs which are not possible to be suppressed by optical filtering, the output electric field after

transmission over optic fiber with a length of L is given by

$$E_{out}=\frac{E_0}{\sqrt{2}}\left\{\sqrt{2}\,J_0^{\,2}(\xi\pi)\cos\left(\omega t+\frac{\pi}{4}\right)-2J_0(\xi\pi)J_1(\xi\pi)\cos\left[\omega t+\Omega_1 t-\beta_1\Omega_1 L-\frac{1}{2}\beta_2\Omega_1^2 L\right]\right.$$

$$-2J_0(\xi\pi)J_1(\xi\pi)\sin\left[\omega t-\Omega_2 t+\beta_1\Omega_2 L-\frac{1}{2}\beta_2\Omega_2^2 L\right]$$

$$+\sqrt{2}J_1^{\,2}(\xi\pi)\sin\left(\omega t+(\Omega_2-\Omega_1)t-\frac{\pi}{4}-\beta_1(\Omega_2-\Omega_1)L-\frac{1}{2}\beta_2(\Omega_2-\Omega_1)^2 L\right)$$

$$-\sqrt{2}J_1^{\,2}(\xi\pi)\sin\left(\omega t-(\Omega_2-\Omega_1)t-\frac{\pi}{4}+\beta_1(\Omega_2-\Omega_1)L-\frac{1}{2}\beta_2(\Omega_2-\Omega_1)^2 L\right)$$

$$+\sqrt{2}J_1^{\,2}(\xi\pi)\sin\left(\omega t+(\Omega_2+\Omega_1)t+\frac{\pi}{4}-\beta_1(\Omega_2+\Omega_1)L-\frac{1}{2}\beta_2(\Omega_2+\Omega_1)^2 L\right)$$

$$-\sqrt{2}J_1^{\,2}(\xi\pi)\sin\left(\omega t-(\Omega_2+\Omega_1)t+\frac{\pi}{4}+\beta_1(\Omega_2+\Omega_1)L-\frac{1}{2}\beta_2(\Omega_2+\Omega_1)^2 L\right)$$

$$+2J_1(\xi\pi)J_2(\xi\pi)\cos\left(\omega t-(2\Omega_2-\Omega_1)t+\beta_1(2\Omega_2-\Omega_1)L-\frac{1}{2}\beta_2(2\Omega_2-\Omega_1)^2 L\right)$$

$$-2J_1(\xi\pi)J_2(\xi\pi)\sin\left(\omega t-(2\Omega_1-\Omega_2)t+\beta_1(2\Omega_1-\Omega_2)L-\frac{1}{2}\beta_2(2\Omega_1-\Omega_2)^2 L\right)$$

$$+\sqrt{2}J_0(\xi\pi)J_2(\xi\pi)\cos\left(\omega t+2\Omega_1 t-\frac{\pi}{4}-2\beta_1\Omega_1 L-2\beta_2\Omega_1^2 L\right)$$

$$+\sqrt{2}J_0(\xi\pi)J_2(\xi\pi)\cos\left(\omega t-2\Omega_1 t-\frac{\pi}{4}+2\beta_1\Omega_1 L-2\beta_2\Omega_1^2 L\right)$$

$$+2J_2^2(\xi\pi)\cos\left(\omega t+2(\Omega_2-\Omega_1)t+\frac{\pi}{4}-2\beta_1(\Omega_2-\Omega_1)L-2\beta_2(\Omega_2-\Omega_1)^2 L\right)$$

$$+2J_2^2(\xi\pi)\cos\left(\omega t-2(\Omega_2-\Omega_1)t+\frac{\pi}{4}+2\beta_1(\Omega_2-\Omega_1)L-2\beta_2(\Omega_2-\Omega_1)^2 L\right)$$

$$-2J_1(\xi\pi)J_3(\xi\pi)\sin\left(\omega t+(3\Omega_1-\Omega_2)t-\frac{\pi}{4}-2\beta_1(3\Omega_1-\Omega_2)L-\frac{1}{2}\beta_2(3\Omega_1-\Omega_2)^2 L\right)$$

$$-2J_1(\xi\pi)J_3(\xi\pi)\sin\left(\omega t-(3\Omega_1-\Omega_2)t-\frac{\pi}{4}+2\beta_1(3\Omega_1-\Omega_2)L-\frac{1}{2}\beta_2(3\Omega_1-\Omega_2)^2L\right)$$

$$+2J_0(\xi\pi)J_1(\xi\pi)\cos\left[\omega t-3\Omega_1 t+3\beta_1\Omega_1 L-\frac{9}{2}\beta_2\Omega_1^2L\right] \quad (2.13)$$

where β_1 and β_2 denote the first and second derivatives of the propagation constant with respect to the optical carrier frequency respectively[17] [18]. The propagation phase shift βL for each optical subcarrier term is different due to the change in the refractive index as a function of the frequency, the subcarrier signal propagates in a fiber link with a group velocity $1/\beta_1$, and the fiber dispersion D is related to the chromatic dispersion parameter β_2 by $D=-2\pi c\beta_2/\lambda^2$, where λ is the operating wavelength and c is the velocity of light in vacuum. The optical spectra for the electric field in (2.13) are shown in Figure 2.4 (a) for the case of Ω_1=4GHz and Ω_2=7GHz.

By photo-detection, the current corresponding to the electric field (2.13) is expressed by

$$I=\Re\eta|E_{out}|^2\approx\frac{\Re\eta|E_0|^2}{2}\left\{J_0^4(\xi\pi)-2\sqrt{2}J_0^3(\xi\pi)J_1(\xi\pi)\cos\left(\Omega_1 t-\beta_1\Omega_1 L-\frac{1}{2}\beta_2\Omega_1^2L-\frac{\pi}{4}\right)\right.$$

$$-2\sqrt{2}J_0^3(\xi\pi)J_1(\xi\pi)\sin\left(\Omega_2 t-\beta_1\Omega_2 L+\frac{1}{2}\beta_2\Omega_2^2L+\frac{\pi}{4}\right)$$

$$+4J_0^2(\xi\pi)J_1^2(\xi\pi)\sin\left(\frac{1}{2}\beta_2(\Omega_2-\Omega_1)^2L\right)\sin[(\Omega_2-\Omega_1)t+\beta_1(\Omega_2-\Omega_1)L]$$

$$-4J_0^2(\xi\pi)J_1^2(\xi\pi)\cos\left(\frac{1}{2}\beta_2(\Omega_2+\Omega_1)^2L\right)\sin[(\Omega_2+\Omega_1)t+\beta_1(\Omega_2+\Omega_1)L]$$

$$-4J_0^2(\xi\pi)J_1^2(\xi\pi)\sin\left((\Omega_2+\Omega_1)t-\beta_1(\Omega_2+\Omega_1)L+\frac{1}{2}\beta_2(\Omega_2^2-\Omega_1^2)L\right)$$

$$\left.-2\sqrt{2}J_0^2(\xi\pi)J_1(\xi\pi)J_2(\xi\pi)\sin\left((2\Omega_1-\Omega_2)t-\beta_1(2\Omega_1-\Omega_2)L-\frac{1}{2}\beta_2(2\Omega_1-\Omega_2)^2L+\frac{\pi}{4}\right)\right.$$

$$+2\sqrt{2}J_0(\xi\pi)J_2(\xi\pi)\cos\left(2\Omega_1 t-\frac{\pi}{2}-2\beta_1\Omega_1 L-2\beta_2\Omega_1^2 L\right)$$

$$+2\sqrt{2}J_0(\xi\pi)J_2(\xi\pi)\cos\left(2\Omega_1 t+\frac{\pi}{2}+2\beta_1\Omega_1 L+2\beta_2\Omega_1^2 L\right)$$

$$+4J_0{}^2(\xi\pi)J_2^2(\xi\pi)\sin\left(2\beta_2(\Omega_2-\Omega_1)^2 L\right)\sin\left(2(\Omega_2-\Omega_1)t-2\beta_1(\Omega_2-\Omega_1)L\right)$$

$$+4J_0(\xi\pi)J_1(\xi\pi)J_2(\xi\pi)J_3(\xi\pi)\cos\left(2(\Omega_2-\Omega_1)t-2\beta_1(\Omega_2-\Omega_1)L-2\beta_2\left(2\Omega_2^2-\Omega_1^2-\Omega_1\Omega_2\right)\right)$$

$$-4J_0(\xi\pi)J_1(\xi\pi)J_3(\xi\pi)\sin\left(\frac{1}{2}\beta_2(3\Omega_1-\Omega_2)^2 L\right)\sin\left((3\Omega_1-\Omega_2)t-2\beta_1(3\Omega_1-\Omega_2)L\right)$$

$$-2\sqrt{2}J_0^3(\xi\pi)J_3(\xi\pi)\cos\left(3\Omega_1 t-3\beta_1\Omega_1 L+\frac{9}{2}\beta_2\Omega_1^2 L+\frac{\pi}{4}\right) \qquad (2.14)$$

The electrical spectra corresponding to (2.14) are shown in Figure 2.4 (b) for the case of Ω_1=4GHz and Ω_2=7GHz. Note that the HD at $2\Omega_1$ and IMD at $2(\Omega_2-\Omega_1)$, which are closer to the RF signal at Ω_2, and IMDs at $(2\Omega_1-\Omega_2)$ and $(\Omega_2-\Omega_1)$, which are closer to RF signal at Ω_1, are dependent on both Ω_1 and Ω_2.

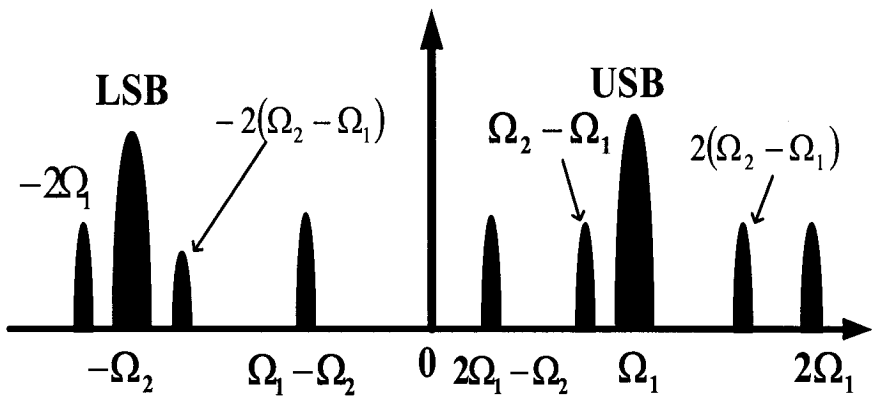

(a)

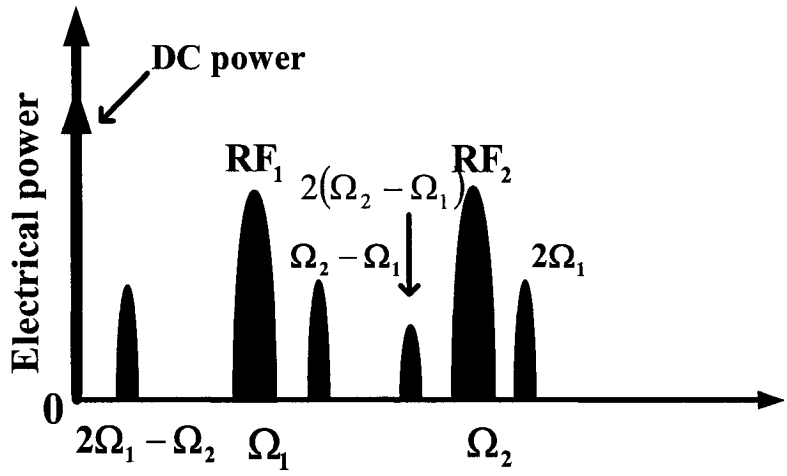

(b)

Figure 2.4 (a) Optical spectra corresponding to (2.12) and (b) electrical spectra corresponding to (2.14), for one optical carrier having TSSB modulation with two optical signal subcarriers at Ω_1 =4 and Ω_2 =7GHz.

Case 1: Suppose that $\Omega_2 = \Omega_1 + 3\,\text{GHz}$, if $\Omega_1 = 4\text{GHz}$ then we have $\Omega_2 = 7\text{GHz}$. Note that frequency Ω_1 cannot be beyond 7GHz and thus Ω_2 is less than 10GHz which is not beyond pass-band of the optical channel spacing of 12.5GHz. If nonlinear distortions are separated in frequency far away from the RF signals, they can be removed by electrical filtering even though such filtering only reduce interference to some extent and does not significantly improve receiver sensitivity. Moreover, very narrow-band electrical filtering does not result in a significant performance improvement. Without loss of generality, we assume that an electrical band-pass filter is used to reduce interference

with a 3dB bandwidth of 2GHz. It is seen that for small Ω_1 and Ω_2 more nonlinear distortions are closer to two RF signals. Thus electrical filtering may not be helpful to reduce them. Figure 2.5 shows the frequency locations of the IMDs and HDs with respect to the frequencies Ω_1 and Ω_2 for $\Omega_2 = \Omega_1 + 3$ GHz. When $\Omega_1 <$ 5GHz, HDs and IMDs at $(2\Omega_1 - \Omega_2)$, $(\Omega_2 - \Omega_1)$, $2\Omega_1$ are closer to RF subcarrier at Ω_1; while $3\Omega_1$, $(\Omega_1 + \Omega_2)$, $(2\Omega_2 - \Omega_1)$ are closer to RF subcarrier at Ω_2. When 5GHz $< \Omega_1 <$ 7GHz, HDs and IMDs at $(2\Omega_1 - \Omega_2)$, $(\Omega_2 - \Omega_1)$, $2(\Omega_2 - \Omega_1)$ are closer RF subcarrier at Ω_1; while $2\Omega_1$ is closer to RF subcarrier at Ω_2.

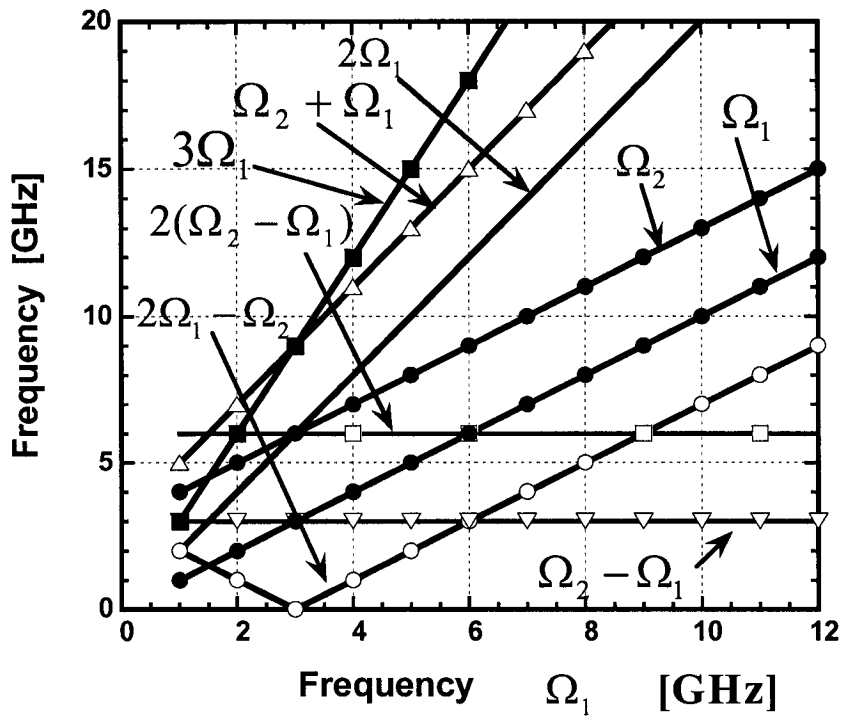

Figure 2.5 The HDs and IMDs frequency locations with respect to RF signals at Ω_1 and Ω_2, in which $\Omega_2 = \Omega_1 + 3$ GHz is supposed.

To study the impact of nonlinear distortions due to HDs and IMDs with fiber dispersion impact, we calculate the noise-to-signal ratio (NSR) to estimate the impact of nonlinear distortion. The reason why we use NSR (instead of the signal-to-noise ratio or SNR) is because nonlinear distortion is noise-like in the system, therefore, NSR is much fit for expressing nonlinear distortion in this system [7]. Based on (2.14), NSR is given in Table 2.1 for different RF frequencies Ω_1 and Ω_2. It is assumed that if nonlinear distortions are out of 12-GHz frequency pass-band, the nonlinear distortions can be removed by optical filtering, and thus that nonlinear distortions are not considered. However, due to limited pass-band of DWDM multiplexer optical carrier and two signal subcarriers may be suppressed. For TSSB modulation, two optical signal subcarriers may have a larger suppression because one of the two optical signal subcarriers is located in one side of the optical carrier and the other in the other side of the optical carrier. Therefore, this suppression is equivalent to decrease of optical modulation index. However, in our analysis we do not consider this suppression of optical modulation index. As shown in Figure 2.4 (b), there are a number of HDs and IMDs in the electrical domain, which degrade both RF signals. One method to show nonlinear distortion impact is to use the ratio of HD or IMD to RF signal in power. Thus there are several ratios for different HDs and IMDs; and it is impossible to have an entire picture of nonlinear distortions. In this thesis, it is assumed that two electrical filters are used to extract the RF signals. We also assume that the electrical filter has 3-dB bandwidth of 2GHz. If nonlinear distortions are within 2GHz pass-band for each RF signal, the nonlinear distortions are considered in

calculation of NSR for that RF signal.

Table 2.1 NSR for one optical carrier having TSSB modulation with different combinations of Ω_1 and Ω_2 and $\Omega_2 = \Omega_1 + 3\,\text{GHz}$.

Ω_1 GHz	Ω_2 GHz	Nonlinear distortion frequencies for Ω_1	Nonlinear distortion frequencies for Ω_2	RF Ω_1 NSR	RF Ω_2 NSR
1	4	$2\Omega_1,\ (\Omega_2 - 2\Omega_1)$	$3\Omega_1, (\Omega_2 - \Omega_1),\ (\Omega_2 + \Omega_1)$	NSR_{1a}	NSR_{2a}
2	5	$(\Omega_2 - \Omega_1),\ (\Omega_2 - 2\Omega_1)$	$3\Omega_1,\ 2\Omega_1,\ 2(\Omega_2 - \Omega_1),$	NSR_{1b}	NSR_{2b}
3-5	6-8	$(\Omega_2 - \Omega_1)$	$2\Omega_1,\ 2(\Omega_2 - \Omega_1)$	NSR_{1c}	NSR_{2c}
6-7	9-10	$2(\Omega_2 - \Omega_1)$	$(3\Omega_1 - \Omega_2)$	NSR_{1d}	NSR_{2d}

NSRs are given by

$$NSR_a = 10\log\left[\frac{2J_0^2(\xi\pi)J_2^2(\xi\pi)\sin^2\left(2\beta_2\Omega_1{}^2L\right)+J_1^2(\xi\pi)J_2^2(\xi\pi)}{J_0^2(\xi\pi)J_1^2(\xi\pi)}\right] \tag{2.15a}$$

$$NSR_{2a} = 10\log\left[\frac{2J_1^4(\xi\pi)\sin^2\left(\frac{1}{2}\beta_2(\Omega_2-\Omega_1)^2L\right)+2J_1^4(\xi\pi)\sin^2\left(\frac{1}{2}\beta_2(\Omega_2+\Omega_1)^2L\right)+J_0^2(\xi\pi)J_3^2(\xi\pi)}{J_0^2(\xi\pi)J_1^2(\xi\pi)}\right] \tag{2.15b}$$

$$NSR_{1b} = 10\log\left[\frac{2J_1^2(\xi\pi)\sin^2\left(\frac{1}{2}\beta_2(\Omega_2-\Omega_1)^2L\right)+J_2^2(\xi\pi)}{J_0^2(\xi\pi)}\right] \tag{2.15c}$$

$$NSR_{2b} = 10\log\left[\frac{J_0^2(\xi\pi)J_2^2(\xi\pi)\sin^2\left(2\Omega_1^2L\right)+2J_2^4(\xi\pi)+J_0^2(\xi\pi)J_3^2(\xi\pi)}{J_0^2(\xi\pi)J_1^2(\xi\pi)}\right] \tag{2.15d}$$

$$NSR_{1c} = 10\log\left[\frac{2J_0^4(\xi\pi)J_1^2(\xi\pi)\sin^2\left(\frac{1}{2}\beta_2(\Omega_2-\Omega_1)^2L\right)+4J_1^2(\xi\pi)J_2^4(\xi\pi)}{J_0^6(\xi\pi)}\right] \quad (2.15e)$$

$$NSR_{2c} = 10\log\left[\frac{J_0^2(\xi\pi)J_2^2(\xi\pi)\sin^2\left(2\Omega_1^2L\right)+2J_2^4(\xi\pi)}{J_0^2(\xi\pi)J_1^2(\xi\pi)}\right] \quad (2.15f)$$

$$NSR_{1d} = 10\log\left[\frac{J_0^2(\xi\pi)J_2^4(\xi\pi)\sin^2\left(2\beta_2(\Omega_2-\Omega_1)^2L\right)+2J_1^2(\xi\pi)J_2^2(\xi\pi)J_3^2(\xi\pi)}{J_0^4(\xi\pi)J_1^2(\xi\pi)}\right] \quad (2.15g)$$

$$NSR_{2d} = 10\log\left[\frac{2J_3^2(\xi\pi)\sin^2\left(\frac{1}{2}\beta_2(3\Omega_1-\Omega_2)^2L\right)}{J_0^2(\xi\pi)}\right] \quad (2.15h)$$

Suppose that fiber has chromatic dispersion of $16\,ps/(nm\cdot km)$, we calculated NSR for optical modulation depths of $\xi\pi$ = 0.1, 1.0, and 1.7, and optical fiber lengths of 0, 25 and 50km, respectively, which are shown in Figure 2.6. It is seen that for $\xi\pi$ of up to 1.0, NSR for RF1 subcarrier is always below -16 dB, as shown in Figure 2.6 (a) and (b). Moreover, for small modulation depth like $\xi\pi$ =0.1 in Figure 2.6 (a) NSR is independent of RF frequencies. With the increase of modulation depth like $\xi\pi$ =1 and 1.7 in Figure 2.6 (b) and (c) NSR increases with fiber length and Ω_1 of up to 8GHz. Particularly, when $\xi\pi$ =1.7, NSR is increased to -8 dB for fiber length of 50 km and Ω_1 of between 6 and 8 GHz. In Figure 2.6 (d), (e) and (f) we calculated NSR for RF signal at Ω_2 with $\Omega_2 = \Omega_1$ +3GHz. It is observed that NSR is decreased with the increase of Ω_2. If $\xi\pi$ =1 or beyond, Ω_2 has be to beyond 9GHz if NSR of -20 dB or less is required.

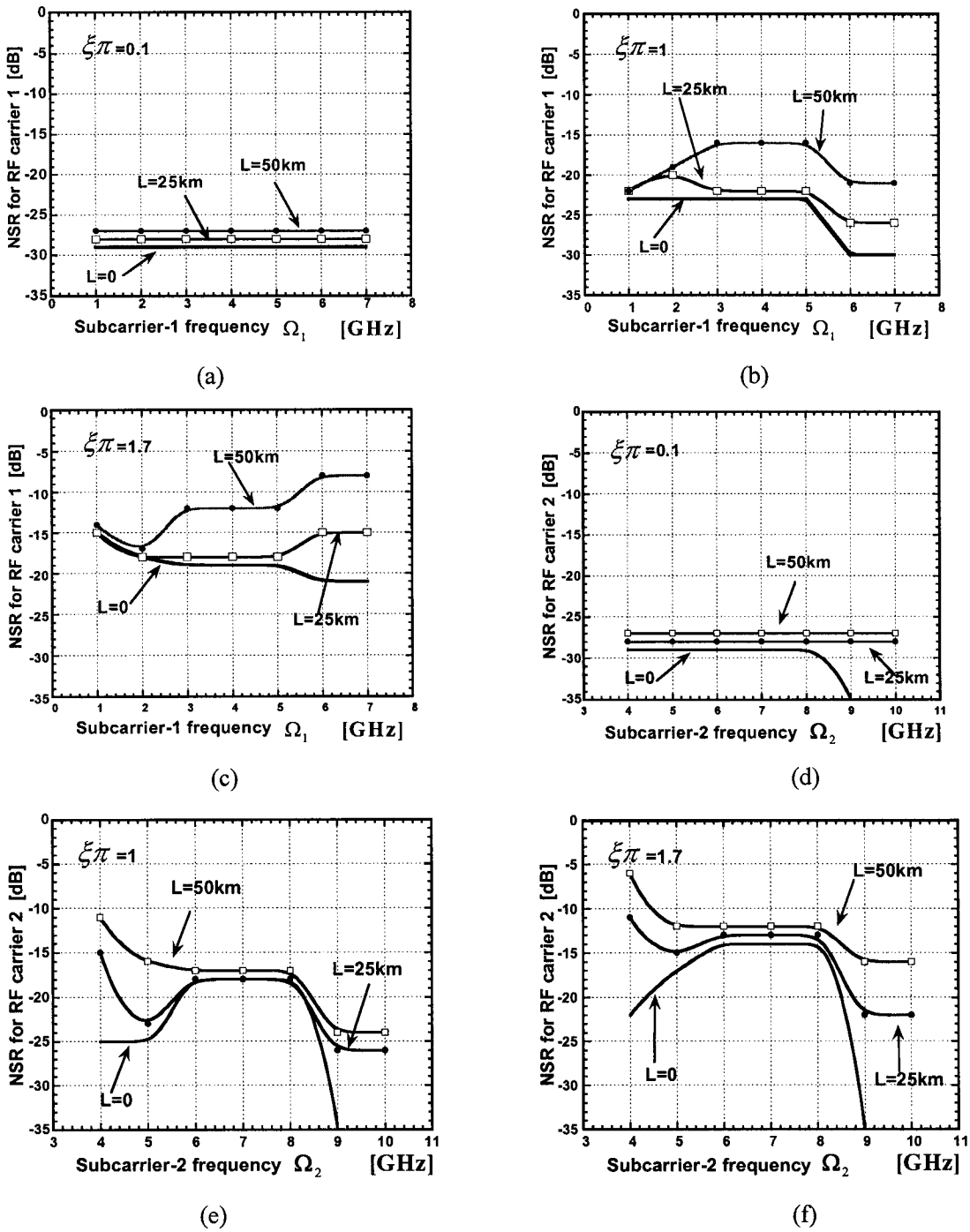

Figure 2.6 Calculated NSR for one optical carrier having TSSB/SCM with modulation depths of $\xi\pi$ =0.1, 1.0, and 1.7 and fiber lengths of 0, 25, and 50 km. NSR of RF signal at Ω_1 with (a) $\xi\pi$ =0.1, (b) $\xi\pi$ =1.0, and (c) $\xi\pi$ =1.7, and NSR of RF signal at Ω_2 with (d) $\xi\pi$ =0.1, (e) $\xi\pi$ =1.0, and (f) $\xi\pi$ =1.7, and an initial Ω_1 =1 GHz used. $\Omega_2 - \Omega_1$ =3 GHz is assumed.

From Figure 2.6, we can know that NSR is strongly dependant on optical modulation depth $\xi\pi$. Here we analyze the relationship between NSR and modulation depth $\xi\pi$, we set the optical fiber length L=50km, Ω_1=4GHz, Ω_2=7GHz, and $\xi\pi$ is changed from 0.1 to 1.7. Figure 2.7 shows that the NSR is increased when the modulation depth $\xi\pi$ increases both for RF1 and RF2.

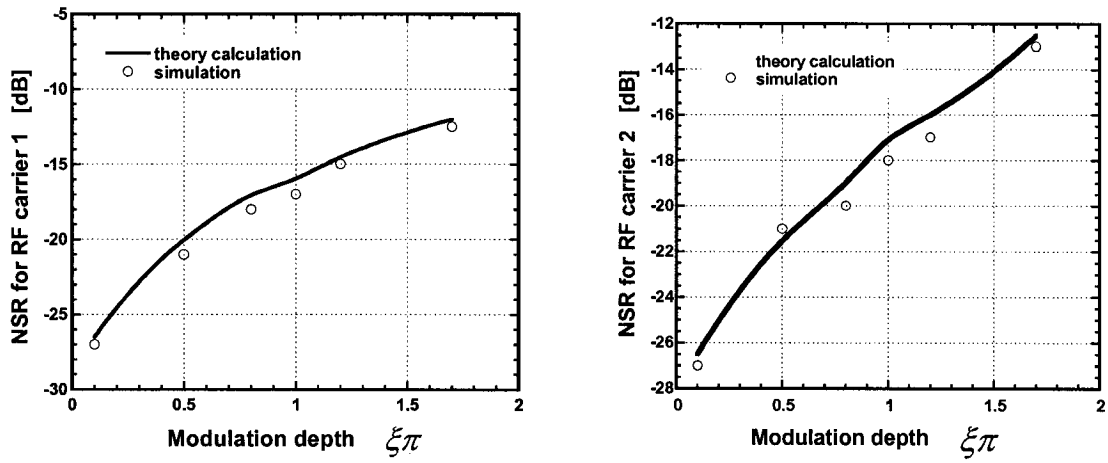

(a) (b)

Figure 2.7 NSR vs. modulation depth for (a) RF at Ω_1 and (b) RF at Ω_2, after optical fiber transmission distance of L=50km, where Ω_1=4 and Ω_2=7GHz are used. Black/dotted line indicates NSR by the theoretical analysis/simulation.

Case 2, when $\Omega_2 = \Omega_1 + 4$ GHz, NSR will be almost the same as Case 1 with $\Omega_2 = \Omega_1 + 3$ GHz when subcarrier Ω_1 is less than 4GHz, however the worse case will happened at $\Omega_1 = 4$ GHz, the IMD $\Omega_2 - \Omega_1 = 4$ GHz will overlap with Ω_1 and $2\Omega_1 = \Omega_2$ will overlap with Ω_2. NSRs will be the same as Case 1 after Ω_1 is bigger than 5GHz.

Case 3, when $\Omega_2 = \Omega_1 + 2$ GHz, NSR will be almost the same as Case 1 with $\Omega_2 = \Omega_1 + 3$ GHz, but some HDs or IMDs will be closer to the optical subcarriers when Ω_1 is from 1GHz to 5GHz, (e.g. if Ω_1=1GHz, and Ω_2=3GHz, then $2\Omega_1$=2GHz is also close to the RF2, if Ω_1=2GHz, and Ω_2=4GHz, then $2\Omega_1$=4GHz will overlap with the RF2).

Case 4, when $\Omega_2 = \Omega_1 + 1$ GHz. It is analyzed in the same way as Case 1. Figure 2.8 (a) shows the optical spectra and Figure 2.8 (b) shows the electrical spectra, where we assumed the Ω_1=3 and Ω_2=4GHz.

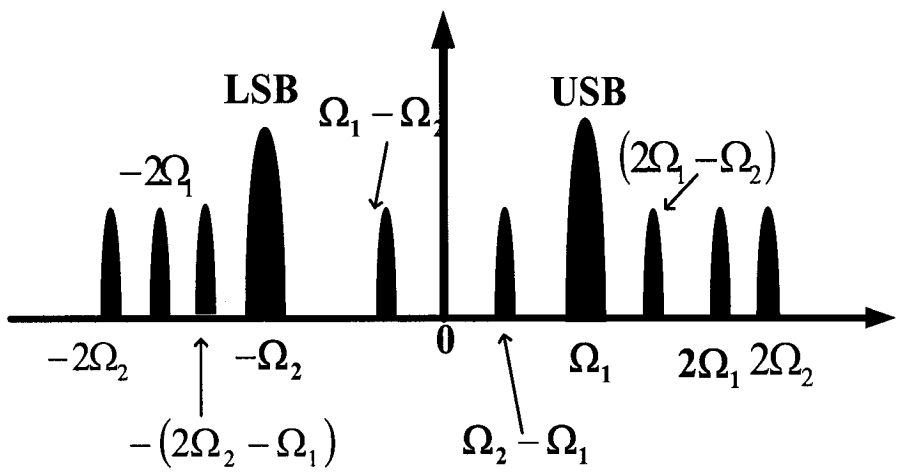

(a)

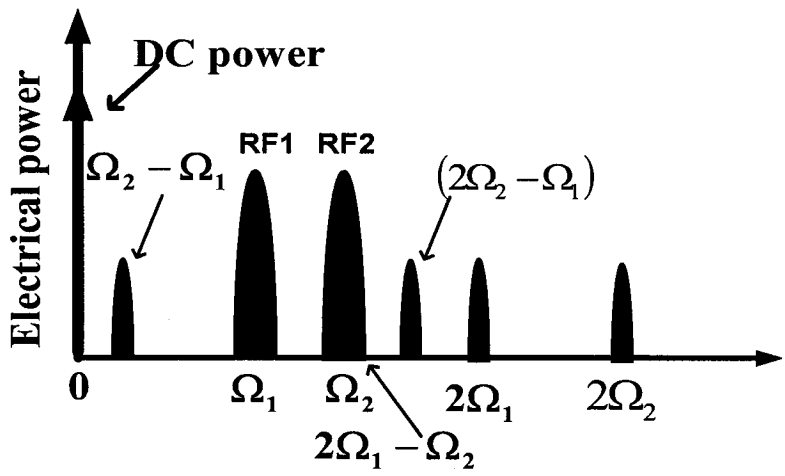

(b)

Figure 2.8 (a) Optical spectra corresponding to (2.12) and (b) Electrical spectra corresponding to (2.14) for one optical carrier having TSSB modulation with two subcarriers at Ω_1=3GHz and Ω_2=4GHz.

Figure 2.9 shows frequency locations of nonlinear HDs and IMDs with RF1 and RF2 subcarrier frequencies. For $\Omega_2=\Omega_1+1\text{GHz}$, it is seen that the HDs or IMDs exist only in one side of each optical subcarrier and there is no HD or IMD between these two subcarriers. In the frequency distribution, the HDs and IMDs at $(2\Omega_1-\Omega_2)$ and $(\Omega_2-\Omega_1)$ are closer to Ω_1, and $(\Omega_1+\Omega_2)$, $(2\Omega_2-\Omega_1)$ and $2\Omega_1$ are closer to Ω_2 when Ω_1 is less than 3GHz. But for Ω_1 equal or bigger than 3GHz, the interference for RF1 subcarrier is $(2\Omega_1-\Omega_2)$, and the interference for the RF2 subcarrier is $(2\Omega_2-\Omega_1)$.

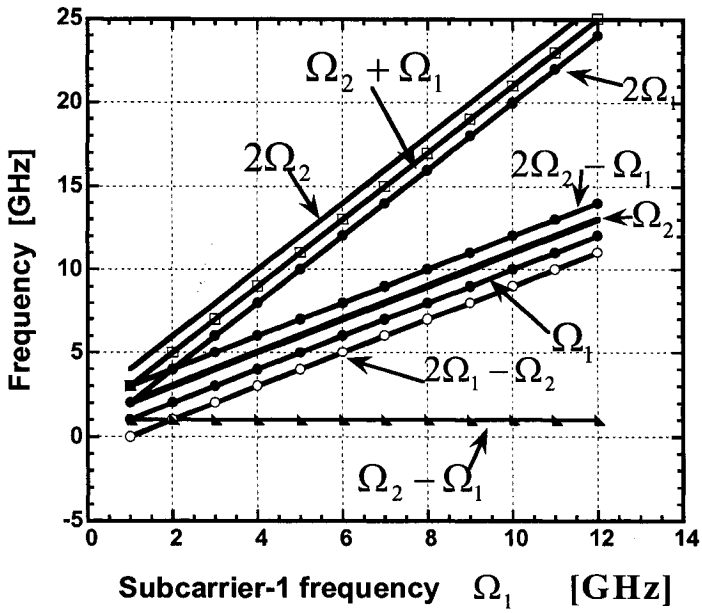

Figure 2.9 HDs and IMDs frequency locations with respect to RF signal frequencies Ω_1 and Ω_2 with $\Omega_2-\Omega_1$=1 GHz.

Suppose the same optical filter is used as in the case of $\Omega_2=\Omega_1+3$ GHz. The HDs and IMDs for different optical subcarrier frequencies Ω_1 and Ω_2, which introduce distortion, are shown in Table 2. Correspondingly, NSR expressions are also given in Table 2.2. But the 3dB bandwidth of the electrical band-pass filter is 2-GHz and only considering the HDs and IMDs as nonlinear distortion.

Table 2.2 NSR for optical carrier having TSSB modulation with different combinations of Ω_1 and Ω_2 with $\Omega_2 - \Omega_1$ =1GHz

Ω_1 [GHz]	Ω_2 [GHz]	Distortion frequency to Ω_1 [GHz]	Distortion frequency to Ω_2 [GHz]	RF Ω_1 NSR	RF Ω_2 NSR
1	2	$(\Omega_2 - \Omega_1), 2\Omega_1$	$2\Omega_1$, $3\Omega_1$, $(\Omega_2 + \Omega_1)$, $(2\Omega_2 - \Omega_1)$	NSR_{3a}	NSR_{4a}
2	3	$(\Omega_2 - \Omega_1)$, $(\Omega_2 - 2\Omega_1)$,	$2\Omega_1$, $(2\Omega_2 - \Omega_1)$	NSR_{3b}	NSR_{4b}
3-9	4-10	$(\Omega_2 - 2\Omega_1)$	$(2\Omega_2 - \Omega_1)$	NSR_{3c}	NSR_{4c}

NSRs are given by

$$NSR_{3a} = 10\log\left[\frac{2J_1^4(\xi\pi)\sin^2\left(\frac{1}{2}\beta_2(\Omega_2-\Omega_1)^2L\right)+J_0^2(\xi\pi)J_2^2(\xi\pi)}{J_0^2(\xi\pi)J_1^2(\xi\pi)}\right] \tag{2.16a}$$

$$NSR_{4a} = 10\log\left[\frac{2J_1^4(\xi\pi)\cos^2\left(\frac{1}{2}\beta_2(\Omega_2+\Omega_1)^2L\right)+J_0^2(\xi\pi)J_2^2(\xi\pi)+J_0^2(\xi\pi)J_3^2(\xi\pi)}{J_0^2(\xi\pi)J_1^2(\xi\pi)}\right] \tag{2.16b}$$

$$NSR_{3b} = 10\log\left[\frac{2J_1^4(\xi\pi)\sin^2\left(\frac{1}{2}\beta_2(\Omega_2-\Omega_1)^2L\right)+J_1^2(\xi\pi)J_2^2(\xi\pi)}{J_0^2(\xi\pi)J_1^2(\xi\pi)}\right] \tag{2.16c}$$

$$NSR_{4b} = 10\log\left[\frac{J_0^2(\xi\pi)J_2^2(\xi\pi)+J_1^2(\xi\pi)J_2^2(\xi\pi)}{J_0^2(\xi\pi)J_1^2(\xi\pi)}\right] \tag{2.16d}$$

$$NSR_{3c} = NSR_{4c} = 10\log\left[\frac{J_2^2(\xi\pi)}{J_0^2(\xi\pi)}\right] \tag{2.16e}$$

Suppose that the fiber has chromatic dispersion of $16\,ps/(nm \cdot km)$, we calculated NSR with optical modulation depths of $\xi\pi$ = 0.1, 1.0, and 1.7, and optical fiber lengths of 0, 25 and 50 km, which are shown in Figure 2.10 respectively, (a) is the NSR for subcarrier at Ω_1 and (b) is the NSR for subcarrier at Ω_2. From Figure 2.10 (a), NSR for RF1 is changing with subcarrier frequency, modulation depth and fiber length when Ω_1 <3GHz, however NSR does not change with RF frequency or fiber length when Ω_1 equal or bigger than 3GHz, and it is around -33dB when the optical modulation depth $\xi\pi$ =0.1. In the same way, NSR for RF2 is not changed with RF frequency and optical fiber length L for Ω_2 =4GHz or higher in Figure 2.10 (b). Compared with Case 1, the nonlinear distortion in this case is smaller than Case 1.

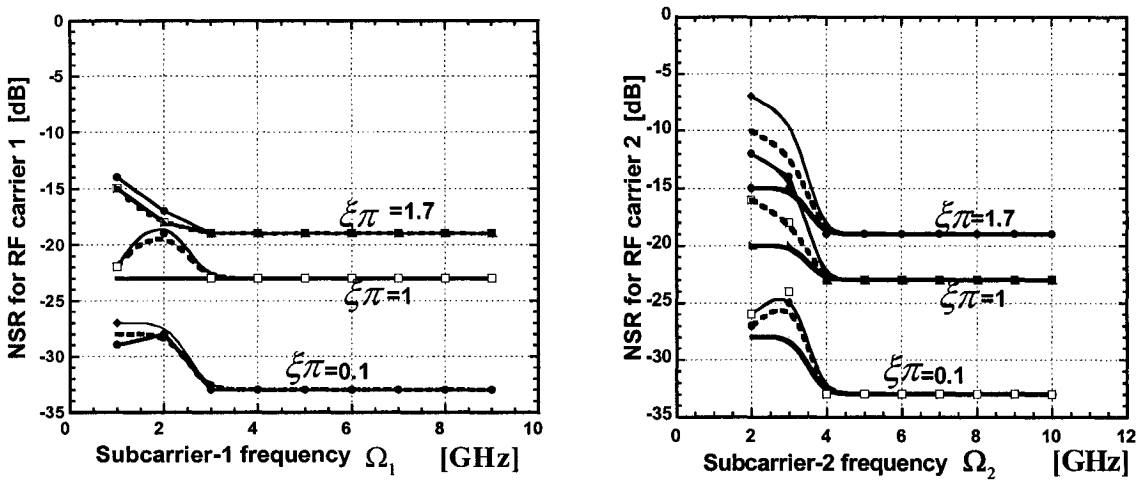

(a) (b)

Figure 2.10 NSR vs. optical subcarrier frequency for (a) Ω_1 and (b) Ω_2, with optical modulation depths of $\xi\pi$ =0.1, $\xi\pi$ =1.0, and $\xi\pi$ =1.7 and optic fiber lengths of 0, 25, and 50 km, (Bold black line, dotted line and tiny line indicate L=0, 25km and 50km). The relation of $\Omega_2 - \Omega_1$ =1GHz is assumed.

2.3 TSSB modulation in DWDM radio over fiber systems

In Section 2.2, we considered nonlinear distortion caused by the two RF signals in the same optical channel.

Then we analyze nonlinear distortion induced by TSSB modulation in DWDM systems [11][20]-[23], since in DWDM systems, there will be many optical channels transmitted in one optical fiber, we use four continual optical channels as an example to analyze nonlinear distortion from the other optical channels, and each optical channel still carries two RF subcarriers. In practical systems, subcarriers may be distributed in the optical channels evenly, we chose the optical channel space of 12.5GHz so that we can use the optical fiber bandwidth efficiently, thus the frequency of the subcarrier must be less than 5GHz. In order to avoid channel interleave, we set the frequency of the RF subcarrier to 4GHz. So in the central station, the data signal is modulated to 4GHz radio frequency, after that, the RF signal is imposed onto the optical carrier, then it can be transmitted to base station. The principle diagram of DWDM radio over fiber system is shown in Figure 2.11.

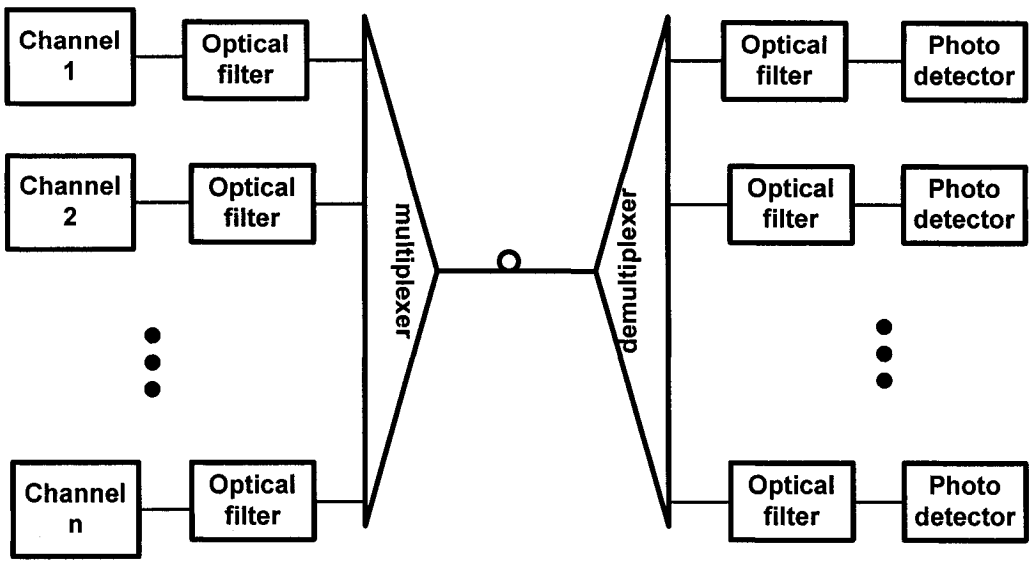

Figure 2.11 The principle diagram of DWDM radio over fiber systems.

The optical channel space is 12.5GHz, the RF frequency is $\Omega_1 = \Omega_2 =$ 4GHz, the frequency difference between the upper-band subcarrier RF1 of the first optical channel and the lower-band subcarrier RF2 of the second optical channel is 4.5GHz, the optical spectral distribution is shown in Figure 2.12, when HDs or IMDs are not considered.

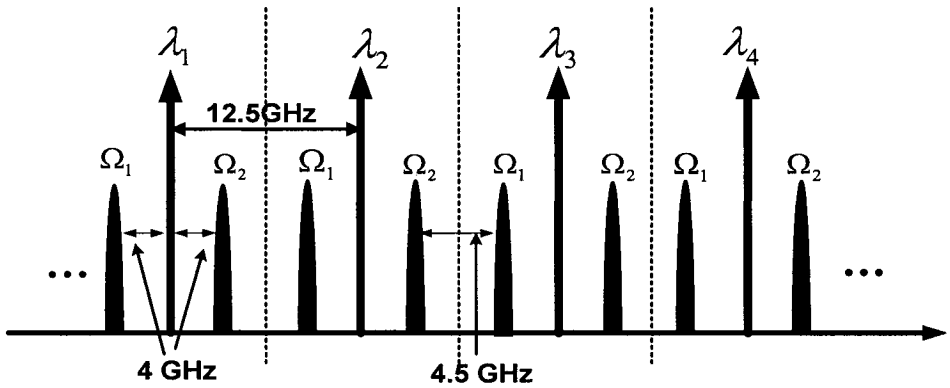

Figure 2.12 The optical spectrum of TSSB modulation in DWDM system

However there are higher-order HDs to interfere the adjacent optical channels. See

Equation (2.12), we use an optical filter with 3dB bandwidth of about 12GHz, then the HDs such as $3\Omega_1$, $3\Omega_2$ or higher-order HDs will be filtered out, and thus we do not consider these distortions.

Besides the nonlinear distortion from the same optical channel, there is nonlinear distortion caused by HDs at $\pm 2\Omega_1$ and $\pm 2\Omega_2$ from the neighbor optical channels. The frequency of the RF1 subcarrier is Ω_1=4GHz, the frequency of HD is $2\Omega_1$=8GHz, and the optical channel space is 12.5GHz, then the HD at $\pm 2\Omega_1$ and $\pm 2\Omega_2$ are 8GHz away from their own optical carrier, but they are near the RF signals of the adjacent optical channels. We use the second optical channel as an example, the second-order HD frequency of the subcarrier is 8GHz, $+2\Omega_1$ and $+2\Omega_2$ are close to the RF1 subcarrier of the third optical channel, $-2\Omega_1$ and $-2\Omega_2$ are close to RF2 subcarrier of the first optical channel. The frequency difference between the subcarrier and the HDs is 0.5 GHz. If we use the optical filter, it is difficult to completely filter out these HDs, due to non-perfect DWDM filters. The optical spectrum is shown on the Figure 2.13.

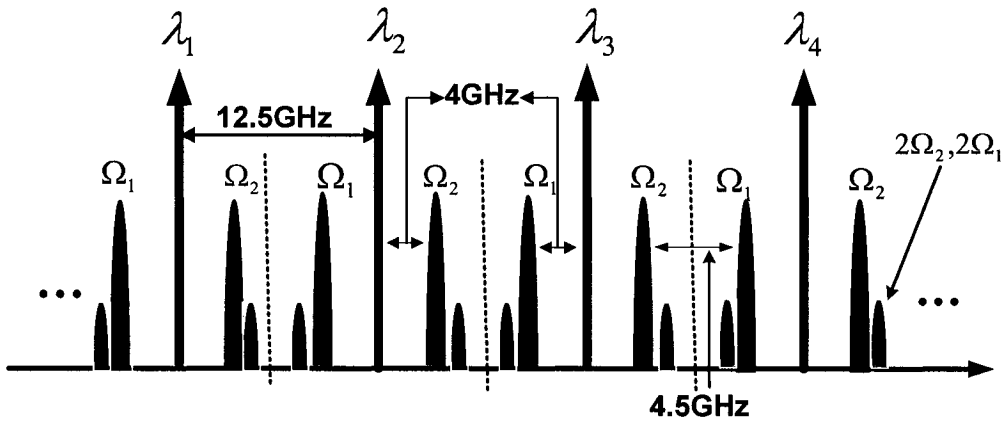

Figure 2.13 The optical spectra with the HDs from the neighbor optical channels in the TSSB modulation in a DWDM system.

From the above example, we know that this second optical channel will cause nonlinear distortion to its neighbor optical channels, i.e. the first and the third optical channel. Now we still use this second optical channel as the example to analyze the nonlinear distortion from the neighbor optical channels.

According to Equation (2.12), the HDs at $+2\Omega_1$ and $+2\Omega_2$ from the first optical channel are 0.5GHz away from the RF1 subcarrier of this second optical channel. In the same way, the HDs at $-2\Omega_1$ and $-2\Omega_2$ from the third optical channel are 0.5GHz away from the RF2 subcarrier of the second optical channel. Suppose these HDs are suppressed by 90% after the optical filtering. Other optical channels get the same interference from the adjacent optical channels. The nonlinear distortion and NSR of TSSB modulation in a DWDM system is shown in Table 2.3.

Table 2.3 NSR for one optical carrier having TSSB/SCM/DWDM modulation with $\Omega_1 = \Omega_2$ =4GHz and the optical channel space is 12.5GHz.

Ω_1 GHz	Ω_2 GHz	Nonlinear distortion frequencies for Ω_1	Nonlinear distortion frequencies for Ω_2	RF Ω_1 NSR	RF Ω_2 NSR
4	4	$2\Omega_1$ and $2\Omega_2$ from neighbor optical channel, $(2\Omega_1 - \Omega_2)$	$2\Omega_1$ and $2\Omega_2$ from neighbor optical channel, $(2\Omega_2 - \Omega_1)$	NSR_1	NSR_2

$$NSR_1 = NSR_2 = 10\log\left[\frac{0.04J_0^2(\xi\pi)J_2^2(\xi\pi)+J_1^2(\xi\pi)J_2^2(\xi\pi)}{J_0^2(\xi\pi)J_1^2(\xi\pi)}\right] \quad (2.17)$$

We consider that the HDs from the neighbor optical channels are reduced to 10% after the optical filtering. Suppose that fiber has chromatic dispersion of $16\,ps/(nm\cdot km)$, we calculate NSR for optical modulation depths of $\xi\pi$ = 0.1, 1.0, and 1.7, and we get the NSR as in Table 2.4.

Table 2.4 NSR for RF1 and RF2 with different modulation depth $\xi\pi$.

$\xi\pi$	NSR for RF1 and RF2
0.1	-24dB
1	-20dB
1.7	-17dB

From the above analysis and Table 2.4, we can know that for $\xi\pi$ = 0.1, the nonlinear distortion for both RF signals is only -24dB, because modulation index is 0.1 and the signal V_m is very small, about 0.159V if we set V_π to 5V, so the HDs or IMDs are very small. For $\xi\pi$ = 1, the nonlinear distortion from both RF signals still can be ignored, the signal V_m will increase to 1.59V, the HDs and the IMDs are also increased, but their impact is not big. For $\xi\pi$ = 1.7, the signal V_m is increased to 2.71V, the HDs and IMDs are largely increased, and nonlinear distortion is considerably increased, which is verified by simulation.

2.4 SSB modulation in single channel radio over fiber systems

The other optical modulation is that one optical wavelength carries two or more RF subcarriers in the same sideband, i.e. upper or lower band. It is called single side band modulation (SSB).

We still use an MZM to generate the SSB modulation. Two sets of the data carried by the microwave carrier. These two RF signals combined and injected to one port of MZM modulator; both signals delayed for 90^0 combined and injected to another port of the MZM modulator. A DC bias voltage is also applied to one electrode while the other is grounded. When a CW electric field of $E_0 e^{-j\omega t}$, ω-optical carrier frequency, is injected into the MZM as Figure 2.14, we have

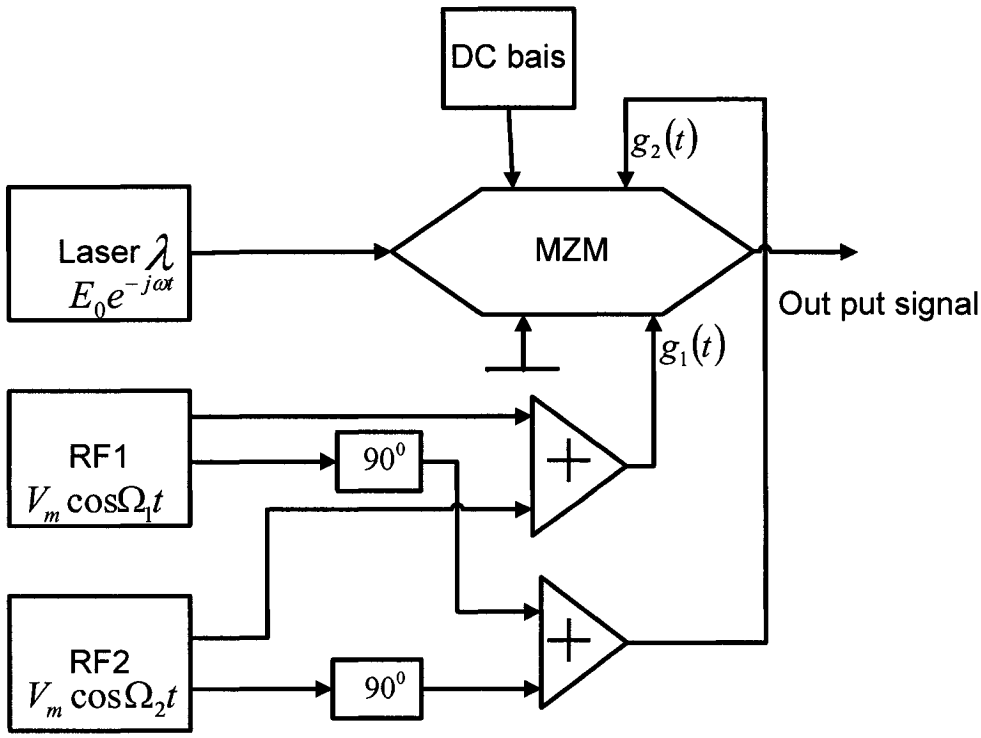

Figure 2.14 The principle diagram of SSB modulation.

$$g_1(t) = V_m(\cos\ \Omega_1 t + \cos\ \Omega_2 t) \tag{2.18}$$

$$g_2(t) = V_m \cos(\Omega_1 t + \pi/2) + V_m \cos(\Omega_2 t + \pi/2) = -V_m(\sin\Omega_1 t + \sin\Omega_2 t) \tag{2.19}$$

$$E_{in} = E_0 e^{-j\omega t} \tag{2.20}$$

For the detailed derivation in Appendix, we get the output electric field due to subcarrier modulation,

$$E_{out} = \frac{E_0}{\sqrt{2}}\left\{\sqrt{2}J_0^{\ 2}(\xi\pi)\cos\left(\omega t + \frac{\pi}{4}\right)\right.$$

$$-2J_0(\xi\pi)J_1(\xi\pi)\cos(\omega t + \Omega_1 t) - 2J_0(\xi\pi)J_1(\xi\pi)\cos(\omega t + \Omega_2 t)$$

$$\left. + \sqrt{2}J_1^{\ 2}(\xi\pi)\cos\left(\omega t + (\Omega_2 - \Omega_1)t - \frac{\pi}{4}\right) + \sqrt{2}J_1^{\ 2}(\xi\pi)\cos\left(\omega t - (\Omega_2 - \Omega_1)t - \frac{\pi}{4}\right)\right.$$

$$-\sqrt{2}J_1^2(\xi\pi)\cos\left(\omega t+(\Omega_2+\Omega_1)t+\frac{\pi}{4}\right)-\sqrt{2}J_1^2(k)\cos\left(\omega t-(\Omega_1+\Omega_2)t+\frac{\pi}{4}\right)$$

$$+\sqrt{2}J_0(\xi\pi)J_2(\xi\pi)\cos\left(\omega t+2\Omega_1 t-\frac{\pi}{4}\right)+\sqrt{2}J_0(\xi\pi)J_2(\xi\pi)\cos\left(\omega t-2\Omega_1 t-\frac{\pi}{4}\right)$$

$$+\sqrt{2}J_0(\xi\pi)J_2(\xi\pi)\cos\left(\omega t+2\Omega_2 t-\frac{\pi}{4}\right)+\sqrt{2}J_0(\xi\pi)J_2(\xi\pi)\cos\left(\omega t-2\Omega_2 t-\frac{\pi}{4}\right)$$

$$+2J_1(\xi\pi)J_2(\xi\pi)\cos(\omega t-(2\Omega_2+\Omega_1)t)+2J_1(\xi\pi)J_2(\xi\pi)\cos(\omega t+(2\Omega_2-\Omega_1)t)$$

$$+2J_1(\xi\pi)J_2(\xi\pi)\cos(\omega t-(2\Omega_1+\Omega_2)t)+2J_1(\xi\pi)J_2(\xi\pi)\cos(\omega t+(2\Omega_1-\Omega_2)t)$$

$$+2J_2^2(\xi\pi)\cos\left(\omega t+2(\Omega_2-\Omega_1)t+\frac{\pi}{4}\right)+2J_2^2(\xi\pi)\cos\left(\omega t-2(\Omega_2-\Omega_1)t+\frac{\pi}{4}\right)$$

$$-2J_1(\xi\pi)J_3(\xi\pi)\cos\left(\omega t+(3\Omega_1-\Omega_2)t-\frac{\pi}{4}\right)-2J_1(\xi\pi)J_3(\xi\pi)\cos\left(\omega t-(3\Omega_1-\Omega_2)t-\frac{\pi}{4}\right)$$

$$+2J_0(\xi\pi)J_3(\xi\pi)\cos(\omega t-3\Omega_1 t)+2J_0(\xi\pi)J_3(\xi\pi)\cos(\omega t-3\Omega_2 t)+\cdots\}$$

(2.21)

In (2.21), the first term denotes the optical carrier, and the second and third terms are two USB subcarriers, and all others are IMDs and HDs. The IMDs occur at $-(\Omega_2-\Omega_1)$, $(\Omega_2-\Omega_1)$, $(2\Omega_2-\Omega_1)$, $(2\Omega_1-\Omega_2)$, $(\Omega_1+\Omega_2)$, $-(\Omega_1+\Omega_2)$, $-(2\Omega_2+\Omega_1)$, $-(2\Omega_1+\Omega_2)$, $2(\Omega_2-\Omega_1)$, $-2(\Omega_2-\Omega_1)$, $-(3\Omega_1-\Omega_2)$ and $(3\Omega_1-\Omega_2)$ etc; and the HDs occur at $2\Omega_1$, $-2\Omega_1$, $2\Omega_2$, $-2\Omega_2$, $-3\Omega_1$, $-3\Omega_2$, etc. For example, suppose that $\Omega_1=4$GHz, and $\Omega_2=7$GHz, thus we have $\pm(\Omega_1-\Omega_2)=\mp3$ GHz, $\pm2(\Omega_2-\Omega_1)=\pm6$GHz, $\pm(\Omega_1+\Omega_2)=\pm11$ GHz, $2\Omega_2-\Omega_1=10$GHz, $2\Omega_1-\Omega_2=1$GHz, $\pm2\Omega_1=\pm8$GHz, and so on. However, if $\Omega_2=2\Omega_1$ and $\Omega_2-\Omega_1=\Omega_1$, this IMD at $\Omega_2-\Omega_1=\Omega_1$ is overlapped with the optical signal RF1 subcarrier, and the HD at $\Omega_2=2\Omega_1$ is overlapped with optical signal RF2 subcarrier. Therefore, the worst nonlinear distortion occurs. If we only

consider the IMDs and HDs which introduce nonlinear distortion near the optical carrier and signal subcarriers, after transmission over optical fiber with a length L [10] [11], we simplify (2.21) into

$$
\begin{aligned}
E_{out} = \frac{E_0}{\sqrt{2}}\Bigg\{ & \sqrt{2}J_0^{\,2}(\xi\pi)\cos\left(\omega t+\frac{\pi}{4}\right) \\
& -2J_0(\xi\pi)J_1(\xi\pi)\cos\left(\omega t+\Omega_1 t-\beta_1\Omega_1 L-\frac{1}{2}\beta_2\Omega_1^2 L\right) \\
& -2J_0(\xi\pi)J_1(\xi\pi)\cos\left(\omega t+\Omega_2 t-\beta_1\Omega_2 L-\frac{1}{2}\beta_2\Omega_2^2 L\right) \\
& +\sqrt{2}J_1^{\,2}(\xi\pi)\cos\left(\omega t+(\Omega_2-\Omega_1)t-\frac{\pi}{4}-\beta_1(\Omega_2-\Omega_1)L-\frac{1}{2}\beta_2(\Omega_2-\Omega_1)^2 L\right) \\
& +\sqrt{2}J_1^{\,2}(\xi\pi)\cos\left(\omega t-(\Omega_2-\Omega_1)t-\frac{\pi}{4}+\beta_1(\Omega_2-\Omega_1)L-\frac{1}{2}\beta_2(\Omega_2-\Omega_1)^2 L\right) \\
& -\sqrt{2}J_1^{\,2}(\xi\pi)\cos\left(\omega t+(\Omega_2+\Omega_1)t+\frac{\pi}{4}-\beta_1(\Omega_2+\Omega_1)L-\frac{1}{2}\beta_2(\Omega_2+\Omega_1)^2 L\right) \\
& -\sqrt{2}J_1^{\,2}(k)\cos\left(\omega t-(\Omega_1+\Omega_2)t+\frac{\pi}{4}+\beta_1(\Omega_2+\Omega_1)L-\frac{1}{2}\beta_2(\Omega_2+\Omega_1)^2 L\right) \\
& +\sqrt{2}J_0(\xi\pi)J_2(\xi\pi)\cos\left(\omega t+2\Omega_1 t-\frac{\pi}{4}-2\beta_1\Omega_1 L-2\beta_2\Omega_1^{\,2}L\right) \\
& +\sqrt{2}J_0(\xi\pi)J_2(\xi\pi)\cos\left(\omega t-2\Omega_1 t-\frac{\pi}{4}+2\beta_1\Omega_1 L-2\beta_2\Omega_1^{\,2}L\right) \\
& +\sqrt{2}J_0(\xi\pi)J_2(\xi\pi)\cos\left(\omega t+2\Omega_2 t-\frac{\pi}{4}-2\beta_1\Omega_2 L-2\beta_2\Omega_2^{\,2}L\right) \\
& +\sqrt{2}J_0(\xi\pi)J_2(\xi\pi)\cos\left(\omega t-2\Omega_2 t-\frac{\pi}{4}+2\beta_1\Omega_2 L-2\beta_2\Omega_2^{\,2}L\right) \\
& +2J_1(\xi\pi)J_2(\xi\pi)\cos\left(\omega t-(2\Omega_2+\Omega_1)t+\beta_1(2\Omega_2+\Omega_1)L-\frac{1}{2}\beta_2(2\Omega_2+\Omega_1)^2 L\right)
\end{aligned}
$$

$$+2J_1(\xi\pi)J_2(\xi\pi)\cos\left(\omega t+(2\Omega_2-\Omega_1)t-\beta_1(2\Omega_2-\Omega_1)L-\frac{1}{2}\beta_2(2\Omega_2-\Omega_1)^2L\right)$$

$$+2J_1(\xi\pi)J_2(\xi\pi)\cos\left(\omega t+(2\Omega_1+\Omega_2)t-\beta_1(2\Omega_1+\Omega_2)L-\frac{1}{2}\beta_2(2\Omega_1+\Omega_2)^2L\right)$$

$$+2J_1(\xi\pi)J_2(\xi\pi)\cos\left(\omega t+(2\Omega_1-\Omega_2)t-\beta_1(2\Omega_1-\Omega_2)L-\frac{1}{2}\beta_2(2\Omega_1-\Omega_2)^2L\right)$$

$$+2J_2^2(\xi\pi)\cos\left(\omega t+2(\Omega_2-\Omega_1)t+\frac{\pi}{4}-2\beta_1(\Omega_2-\Omega_1)L-2\beta_2(\Omega_2-\Omega_1)^2L\right)$$

$$+2J_2^2(\xi\pi)\cos\left(\omega t-2(\Omega_2-\Omega_1)t+\frac{\pi}{4}+2\beta_1(\Omega_2-\Omega_1)L-2\beta_2(\Omega_2-\Omega_1)^2L\right)$$

$$-2J_1(\xi\pi)J_3(\xi\pi)\cos\left(\omega t+(3\Omega_1-\Omega_2)t-\frac{\pi}{4}-2\beta_1(3\Omega_1-\Omega_2)L-\frac{1}{2}\beta_2(3\Omega_1-\Omega_2)^2L\right)$$

$$-2J_1(\xi\pi)J_3(\xi\pi)\cos\left(\omega t-(3\Omega_1-\Omega_2)t-\frac{\pi}{4}+2\beta_1(3\Omega_1-\Omega_2)L-\frac{1}{2}\beta_2(3\Omega_1-\Omega_2)^2L\right)$$

(2.22)

In the same way as for TSSB modulation, it is supposed that the high-order harmonic and inter-modulation distortions, which are out-of 12-GHz pass-band, can be removed by optical filtering. However, for the SSB modulation both optical signal RF1 and RF2 subcarriers are in the same side of the optical carrier [15]. We use an optical pass-band filter to get the optical carrier and signal subcarriers. We set the bandwidth of the optical filter is 12-GHz, so that the optical carrier and signal subcarriers will not be affected by the filtering, it can be seen on Figure 2.15 (a). In the electrical field, as the same in TSSB, we use the electrical filter with 3dB bandwidth is 2GHz.

Suppose that $\Omega_2 - \Omega_1 = 3\,\text{GHz}$, the optical spectra corresponding to (2.22) are shown in Figure 2.15 (a). After optical filtering and photo-detection, the current can be written as

$$I = \Re\eta|E_{out}|^2 \approx \frac{\Re\eta|E_0|^2}{2}\left\{J_0{}^4(\xi\pi) - 2\sqrt{2}J_0{}^3(\xi\pi)J_1(\xi\pi)\cos\left(\Omega_1 t - \beta_1\Omega_1 L - \frac{1}{2}\beta_2\Omega_1{}^2 L - \frac{\pi}{4}\right)\right.$$

$$-2\sqrt{2}J_0{}^3(\xi\pi)J_1(\xi\pi)\cos\left(\Omega_2 t - \beta_1\Omega_2 L - \frac{1}{2}\beta_2\Omega_2{}^2 L - \frac{\pi}{4}\right)$$

$$+4J_0^2(\xi\pi)J_1^2(\xi\pi)\cos\left(\frac{\pi}{4} - \frac{1}{2}\beta_2(\Omega_1^2 + \Omega_1\Omega_2)L\right)\cos\left((\Omega_2 - \Omega_1)t - \beta_1(\Omega_2 - \Omega_1)L - \frac{1}{2}\beta_2(\Omega_2^2 - \Omega_1\Omega_2)L - \frac{\pi}{4}\right)$$

$$-4J_0{}^2(\xi\pi)J_1{}^2(\xi\pi)\cos((\Omega_2 + \Omega_1)t - \beta_1(\Omega_2 + \Omega_1)L)$$

$$+4J_0{}^3(\xi\pi)J_2(\xi\pi)\cos\left(2\Omega_1 t - 2\beta_1\Omega_1 L - 2\beta_2\Omega_1{}^2 L - \frac{\pi}{2}\right)$$

$$+2\sqrt{2}J_0{}^2(\xi\pi)J_1(\xi\pi)J_2(\xi\pi)\cos\left((2\Omega_2 - \Omega_1)t - \beta_1(2\Omega_2 - \Omega_1)L + \frac{1}{2}\beta_2(2\Omega_2 - \Omega_1)^2 L + \frac{\pi}{4}\right)$$

$$+2\sqrt{2}J_0{}^2(\xi\pi)J_1(\xi\pi)J_2(\xi\pi)\cos\left((2\Omega_1 - \Omega_2)t - \beta_1(2\Omega_1 - \Omega_2)L + \frac{1}{2}\beta_2(2\Omega_1 - \Omega_2)^2 L + \frac{\pi}{4}\right)$$

$$+2\sqrt{2}J_0{}^2(\xi\pi)J_1(\xi\pi)J_2(\xi\pi)\cos\left((2\Omega_1 + \Omega_2)t - \beta_1(2\Omega_1 - \Omega_2)L - \frac{1}{2}\beta_2(2\Omega_1 - \Omega_2)^2 L - \frac{\pi}{4}\right)$$

$$+4J_0{}^2(\xi\pi)J_2^2(\xi\pi)\cos\left(2(\Omega_2 - \Omega_1)t - 2\beta_1(\Omega_2 - \Omega_1)L - 2\beta_2(\Omega_2 - \Omega_1)^2 L\right)$$

$$\left.-4J_0^2(\xi\pi)J_1(\xi\pi)J_3(\xi\pi)\cos\left((3\Omega_1 - \Omega_2)t - 2\beta_1(3\Omega_1 - \Omega_2)L - \frac{1}{2}\beta_2(3\Omega_1 - \Omega_2)^2 L - \frac{\pi}{4}\right)\right. \quad (2.23)$$

Figure 2.15(b) is the electrical spectra corresponding to (2.23), and Figure 2.16 shows the frequency locations of the IMDs and HDs with respect to the frequencies Ω_1 and Ω_2 with $\Omega_2 = \Omega_1 + 3\,\text{GHz}$. It is found that an additional IMD at $\Omega_2 - \Omega_1$ will introduce nonlinear distortion for Ω_1 of 2-6 GHz. We can see that the HDs and IMDs at $(2\Omega_1 - \Omega_2)$, $(\Omega_2 - \Omega_1)$, $2\Omega_1$ are close to the Ω_1, and IMDs at $(\Omega_1 + \Omega_2)$, $(2\Omega_2 - \Omega_1)$

are close to RF signal at Ω_2 when Ω_1 is less than 5GHz. IMDs at $(2\Omega_1 - \Omega_2)$, $(\Omega_2 - \Omega_1)$, $2(\Omega_2 - \Omega_1)$ are close to RF signal at Ω_1, HD at $2\Omega_1$ is close to RF signal at Ω_2 for $5\text{GHz} < \Omega_1 < 7\text{GHz}$.

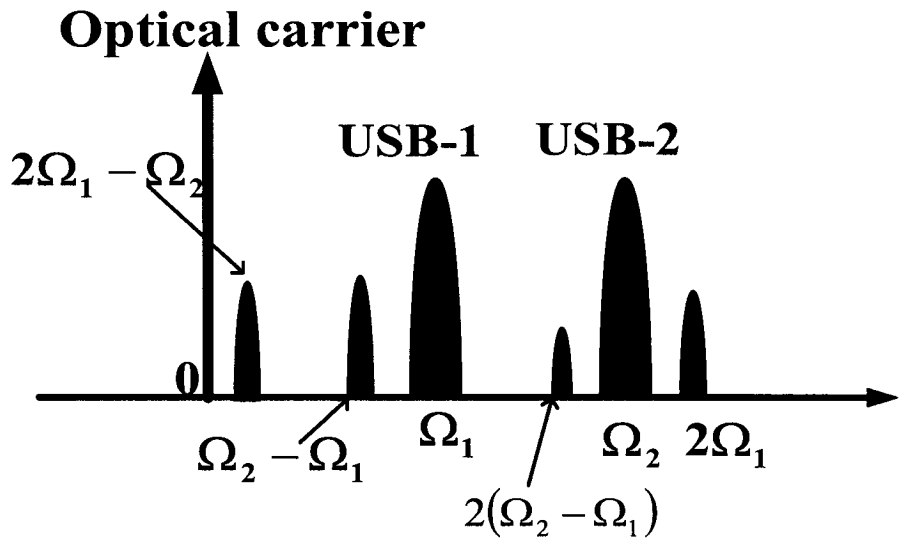

(a)

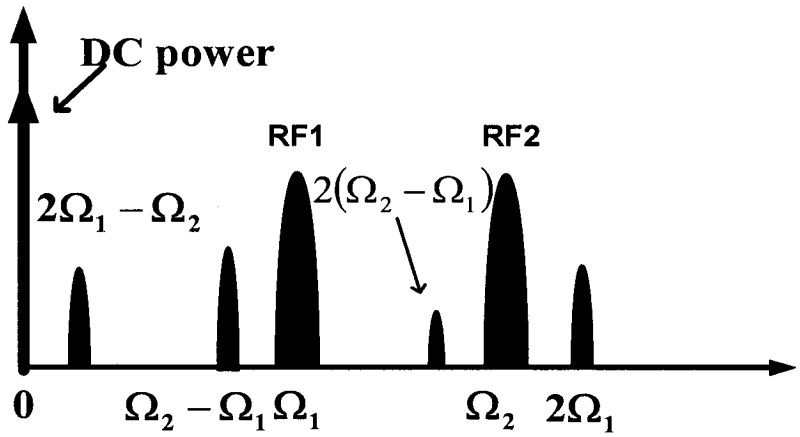

(b)

Figure 2.15 (a) Optical spectra corresponding to (2.21) and (b) Electrical spectra corresponding to (2.23) for one optical carrier having SSB modulation with two subcarrier signals Ω_1=4GHz and Ω_2=7GHz.

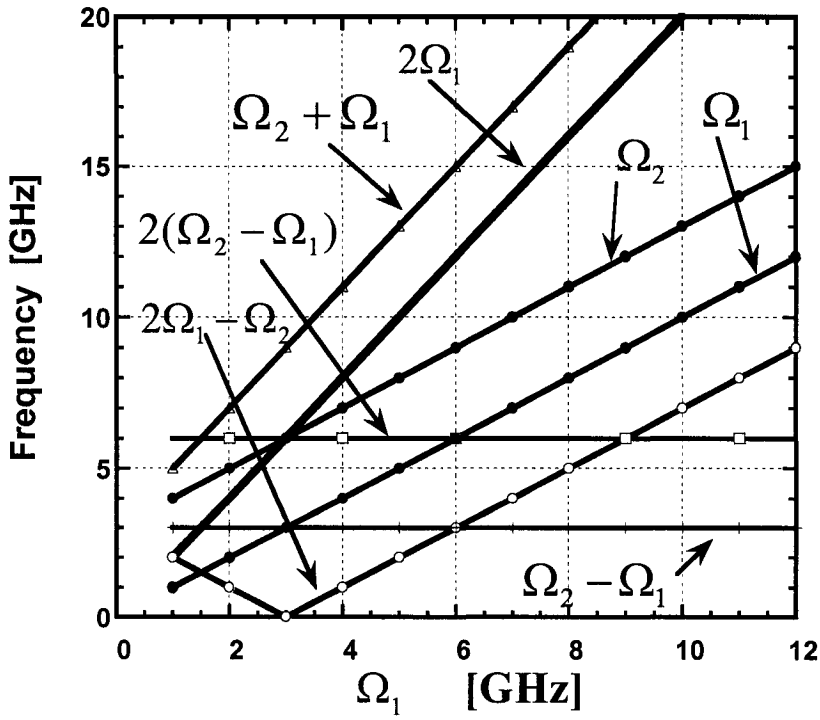

Figure 2.16 The HDs and IMDs frequency locations with respect to RF signals at Ω_1 and Ω_2 and $\Omega_2 = \Omega_1 + 3$ GHz is supposed.

We also study the impact of nonlinear distortions due to HDs and IMDs with fiber dispersion impact, and calculated the noise-to-signal ratio (NSR) to estimate the impact of nonlinear distortion. Based on (2.23), the NSR is given in Table 2.5 for different subcarrier frequency Ω_1 and Ω_2.

Table 2.5 NSR for optical carrier having SSB modulation with different combinations of Ω_1 and Ω_2 with $\Omega_2 = \Omega_1 + 3\,\text{GHz}$

Ω_1 GHz	Ω_2 GHz	Distortion Frequency to Ω_1 [GHz]	Distortion Frequency to Ω_2 [GHz]	RF Ω_1 NSR	RF Ω_2 NSR
1	4	$2\Omega_1$, $(\Omega_2 - 2\Omega_1)$	$(\Omega_2 - \Omega_1)$, $(\Omega_2 + \Omega_1)$	NSR_{5a}	NSR_{6a}
2	5	$(\Omega_2 - \Omega_1)$, $(\Omega_2 - 2\Omega_1)$	$2\Omega_1$, $2(\Omega_2 - \Omega_1)$,	NSR_{5b}	NSR_{6b}
3-5	6-8	$(\Omega_2 - \Omega_1)$	$2\Omega_1$, $2(\Omega_2 - \Omega_1)$	NSR_{5c}	NSR_{6b}
6-7	9-10	$2(\Omega_2 - \Omega_1)$	$(3\Omega_1 - \Omega_2)$	NSR_{5d}	NSR_{6c}

NSRs are given by

$$NSR_{5a} = 10\log\left[\frac{2J_0^2(\xi\pi)J_2^2(\xi\pi) + J_1^2(\xi\pi)J_2^2(\xi\pi)}{J_0^2(\xi\pi)J_1^2(\xi\pi)}\right] \tag{2.24a}$$

$$NSR_{6a} = 10\log\left[\frac{2J_1^2(\xi\pi)}{J_0^2(\xi\pi)}\right] \tag{2.24b}$$

$$NSR_{5b} = 10\log\left[\frac{2J_1^2(\xi\pi)\cos^2\left(\frac{\pi}{4} - \frac{1}{2}\beta_2(\Omega_1^2 + \Omega_1\Omega_2)L\right) + J_2^2(\xi\pi)}{J_0^2(\xi\pi)}\right] \tag{2.24c}$$

$$NSR_{6b} = 10\log\left[\frac{2J_0^2(\xi\pi)J_2^2(\xi\pi) + 2J_2^4(\xi\pi)}{J_0^2(\xi\pi)J_1^2(\xi\pi)}\right] \tag{2.24d}$$

$$NSR_{5c} = 10\log\left[\frac{2J_1^2(\xi\pi)\cos^2\left(\frac{\pi}{4} - \frac{1}{2}\beta_2(\Omega_1^2 + \Omega_1\Omega_2)L\right)}{J_0^2(\xi\pi)}\right] \tag{2.24e}$$

$$NSR_{6c} = 10\log\left[\frac{2J_3^2(\xi\pi)}{J_0^2(\xi\pi)}\right] \tag{2.24f}$$

$$NSR_{5d} = 0\log\left[\frac{2J_2^4(\xi\pi)}{J_0^2(\xi\pi)J_1^2(\xi\pi)}\right] \tag{2.24g}$$

Suppose that fiber has chromatic dispersion of $16\,ps/(nm\cdot km)$, we calculate NSR for optical modulation depths of $\xi\pi = 0.1$, 1.0, and 1.7, and fiber lengths of 0, 25 and 50 km, which are shown in Figure 2.17, respectively. Figure 2.17 (a) shows that NSR for subcarrier signal at Ω_1 is -27dB and not changing with RF frequency and optical fiber length L when modulation depth $\xi\pi$=0.1. But when $\xi\pi$=1 and 1.7, NSR is increased largely and is also changed with optical fiber length L and frequency Ω_1, as seen from Figure 2.17 (b) and (c). From Figure 2.17 (d), NSR for subcarrier signal at Ω_2 is dependent on the modulation depth $\xi\pi$ and frequency Ω_2, and is independent of the optical fiber length L.

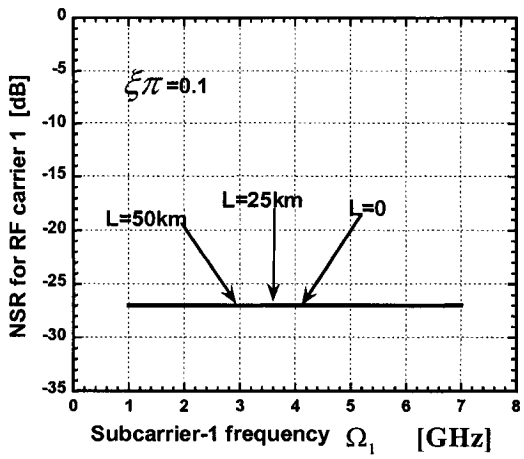

(a)

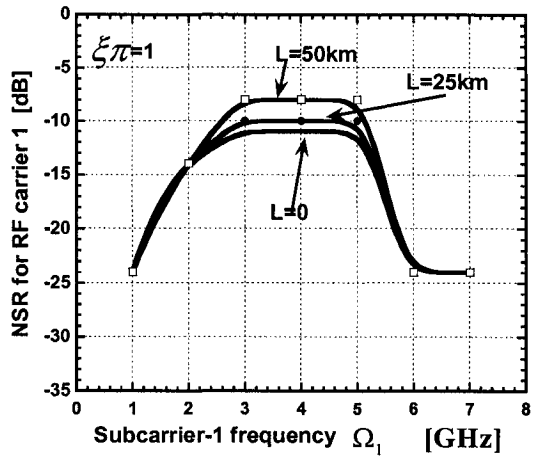

(b)

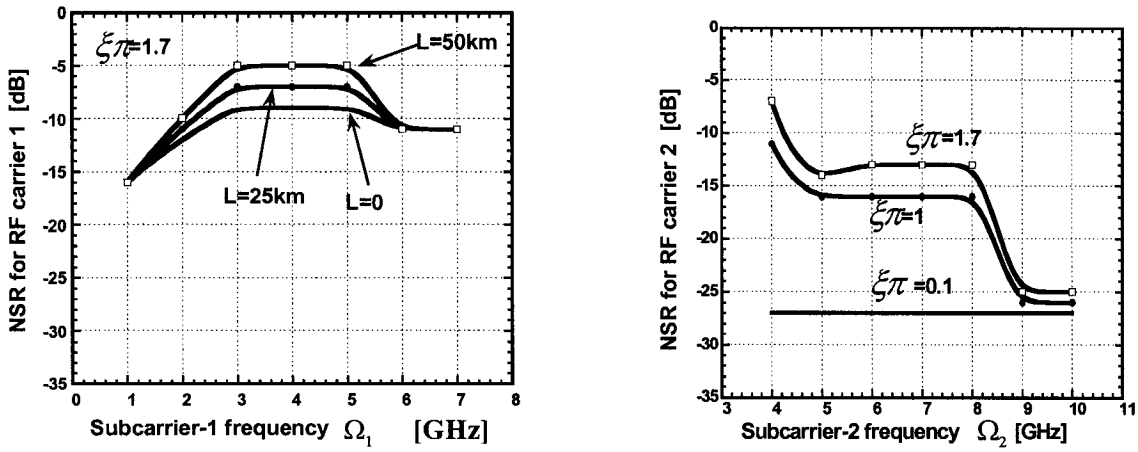

(c) (d)

Figure 2.17 Calculated NSRs for optical carrier having SSB modulation with two subcarrier signals (both in the same side band) with modulation depths of $\xi\pi$ =0.1, $\xi\pi$ =1.0, and $\xi\pi$ =1.7 and fiber lengths of 0, 25, and 50 km. NSR for RF signal at Ω_1 with (a) $\xi\pi$ =0.1, (b) $\xi\pi$ =1.0, and (c) $\xi\pi$ =1.7, and (d) NSR for RF signal at Ω_2 with the above $\xi\pi$. The relation of $\Omega_2 = \Omega_1 + 3\,\text{GHz}$ is assumed.

From Figure 2.17, we can know that the NSR is strongly dependant on the optical modulation depth $\xi\pi$. So we also analyzed the relationship between the NSR and the $\xi\pi$. In order to be compared with the TSSB modulation, we set the same optical length of L=50km, Ω_1=4GHz, Ω_2=7GHz, and $\xi\pi$ is changed from 0.1 to 1.7. Figure 2.18 shows that NSR is increased with the modulation depth.

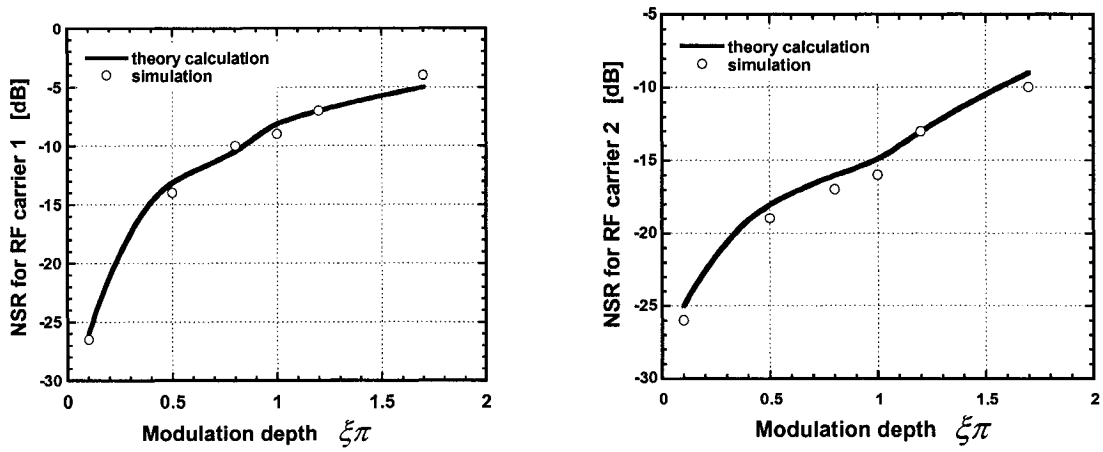

(a) (b)

Figure 2.18 NSR vs. modulation depth for (a) RF at Ω_1 and (b) RF at Ω_2, after fiber transmission distance of L=50km, where Ω_1=4GHz and Ω_2=7GHz are used. Black/dotted line indicates NSR by the theoretical analysis/simulation.

If $\Omega_2 = \Omega_1 + 4$ GHz, the NSR will be almost the same as $\Omega_2 = \Omega_1 + 3$ GHz when subcarrier Ω_1 is less than 4GHz. However the worse case will happen for $\Omega_1 = 4$ GHz, the IMD at $\Omega_2 - \Omega_1 = 4$ GHz will overlap with Ω_1 and HD at $2\Omega_1 = \Omega_2$ will overlap with Ω_2; and the NSRs will be the same for Ω_1 of bigger than 5GHz.

If $\Omega_2 = \Omega_1 + 2$ GHz, the NSR will be almost the same as for $\Omega_2 = \Omega_1 + 3$ GHz case, the difference is some HDs or IMDs which will be close to the optical subcarriers when Ω_1 is from 1 to 5GHz, (e.g. if Ω_1=1GHz, and Ω_2=3GHz, then $2\Omega_1$=2GHz is also close to the RF2 subcarrier, and if Ω_1=2GHz, and Ω_2=4GHz, then $2\Omega_1$=4GHz will overlap the RF2 subcarrier).

However if $\Omega_2 - \Omega_1$ =1GHz, there is small nonlinear distortion interference for RF1 and RF2 for Ω_1=3 GHz and higher. The distortion is the same as in TSSB modulation, because the HDs and IMDs will be distributed the same after optical filtering.

2.5 SSB modulation in DWDM radio over fiber systems

In order to compare with TSSB modulation we chose Ω_1= 4 GHz and Ω_2= 8.5 GHz. Then the optical carriers' and subcarriers' distribution in the DWDM system is the same as for TSSB modulation. Since it is the SSB modulation in DWDM system [11][20]-[23] for each optical channel, the subcarriers are distributed at the same side of the optical carrier. If we set them in the upper-band side, the optical spectrum of the SSB/DWDM is shown in Figure 2.19.

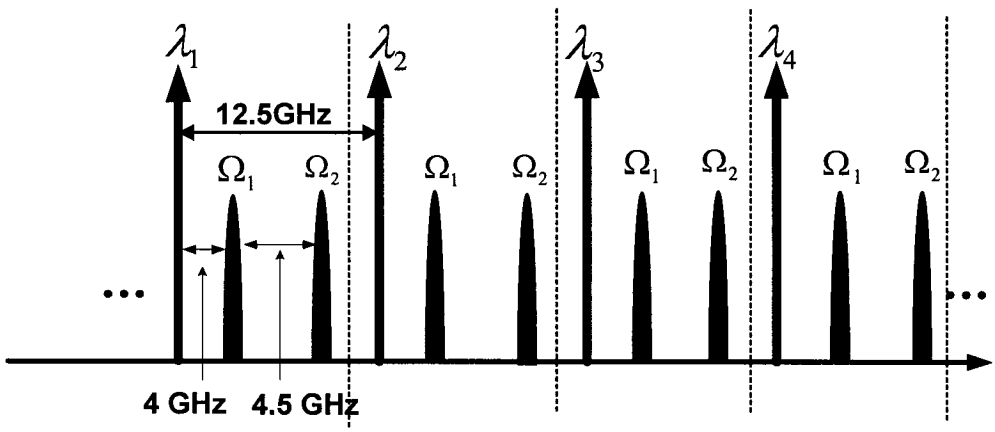

Figure 2.19 The optical spectra of SSB modulation in DWDM system.

As we analyzed in Section 2.4, the main nonlinear distortion for RF1 subcarrier is IMD at Ω_2-Ω_1 which is from the same optical channel, however, IMD at $-(\Omega_2-\Omega_1)$ is close to RF2 subcarrier of the neighbor optical channel, because this IMD at $\pm(\Omega_2-\Omega_1)$= $\pm$4.5GHz is located in two-sides of the optical spectrum. On the other hand, HDs at $\pm 2\Omega_1$= $\pm$8GHz are located in two-sides of the optical spectrum, HD at $+2\Omega_1$ is near the RF2 subcarrier in the same optical channel and HD at $-2\Omega_1$ is close to RF1 subcarrier in the neighbor optical channel. We still use 4 adjacent optical channels as an example, and Fig. 2.20 is the optical spectra diagram.

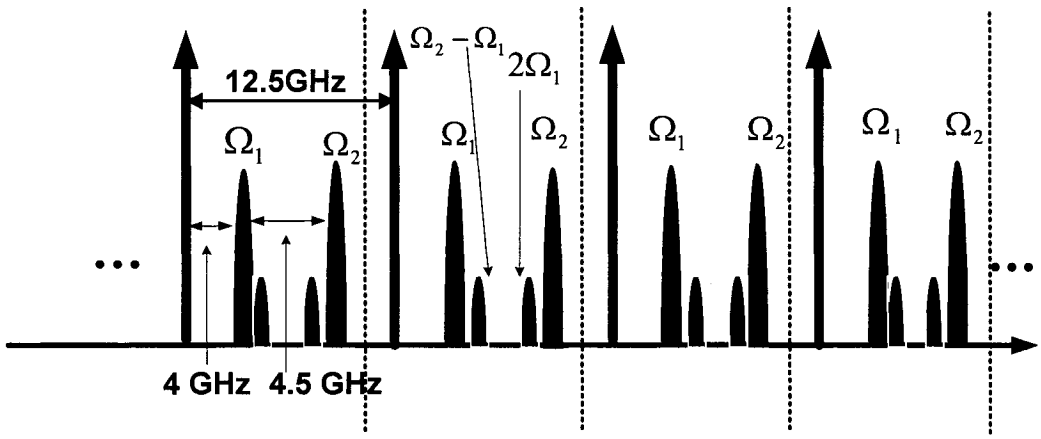

Figure 2.20 The optical spectra with the nonlinear distortion of SSB modulation in a DWDM system.

Here are 4 adjacent optical channels in a DWDM transmission system shown as in Figure2.20. We considered the second optical channel as an example to analyze the nonlinear distortion including from the neighbor optical channels. For the RF1 subcarrier,

there is IMD at $(\Omega_2 - \Omega_1)$ from the same optical channel, and HD at $+2\Omega_2$ from the first optical channel at $+2\Omega_2$=17GHz. If the optical channel space is 12.5GHz, it is 0.5GHz away from the RF1 subcarrier of the second optical channel. The RF2 subcarrier may interfere with the HD at $+2\Omega_1$ from the same optical channel, may also interfere with the IMD at $-(\Omega_2 - \Omega_1)$ from the third optical channel. Since we use an optical filter to filter out the HDs or IMDs before all optical channels were combined by the multiplexer, the interference from the neighbor optical channel can be decreased, and we consider 10% of the HD or IMD from the neighbor optical channels which affect this optical channel after the optical filtering. In the same way, all the other optical channels obtain the same interference from the neighbor optical channels. Nonlinear distortion and NSR of SSB modulation in a DWDM system is shown in Table 2.6.

Table 2.6 NSR for one optical carrier having SSB/SCM/DWDM modulation with Ω_1 = 4GHz and Ω_2=8.5GHz and the optical channel space is 12.5GHz.

Ω_1 GHz	Ω_2 GHz	Nonlinear distortion frequencies for Ω_1	Nonlinear distortion frequencies for Ω_2	RF Ω_1 NSR	RF Ω_2 NSR
4	8.5	$(\Omega_2 - \Omega_1)$, $2\Omega_2$ from neighbor optical channel	$2\Omega_1$, $-(\Omega_2 - \Omega_1)$ from neighbor optical channel	NSR_3	NSR_4

$$NSR_3 = 10\log\left[\frac{J_1^4(\xi\pi)+0.01J_0^2(\xi\pi)J_2^2(\xi\pi)}{J_0^2(\xi\pi)J_1^2(\xi\pi)}\right] \tag{2.25}$$

$$NSR_4 = 10\log\left[\frac{0.01J_1^4(\xi\pi)+J_0^2(\xi\pi)J_2^2(\xi\pi)}{J_0^2(\xi\pi)J_1^2(\xi\pi)}\right] \tag{2.26}$$

Suppose that fiber has chromatic dispersion of $16\,ps/(nm\cdot km)$, we calculate NSR for optical modulation depths of $\xi\pi$ = 0.1, 1.0, and 1.7, we got the nonlinear distortion in SSB/DWDM as in Table 2.7.

Table 2.7 NSR for RF1 and RF2 with different modulation depth $\xi\pi$.

$\xi\pi$	NSR for RF1	NSR for RF2
0.1	-24dB	-24dB
1	-10dB	-15dB
1.7	-5	-10dB

When $\xi\pi$ = 0.1, the NSR for RF1 and RF2 are almost none, because the signal is very small, the HDs or IMDs are much more small, which can be ignored. When $\xi\pi$ = 1, the NSR for both RF1 and RF2 are increased, since the IMD at $(\Omega_2 - \Omega_1)$ is bigger than the HDs at $2\Omega_2$ or $2\Omega_1$, so NSR for RF1 is bigger than the NSR for RF2. Then when $\xi\pi$ = 1.7, the nonlinear distortion is the biggest, especially for the RF1, such interference is unbearable. They are verified by the simulations.

2.6 Summary

The optical subcarrier modulation will generate nonlinear distortion. Nonlinear distortion will interfere with the signal subcarriers if one wavelength carrys two or more subcarriers either in TSSB or SSB modulation. Such nonlinear distortion is harmonic distortion and inter-modulation distortion caused by the MZM nonlinear transfer function. With the theoretical analysis and numerical calculations, the NSR of the nonlinear distortion is dependant on the subcarrier frequency Ω_1 and Ω_2, optical modulation depth $\xi\pi$ and optical fiber length L. Even with the same subcarrier frequency, optical modulation depth $\xi\pi$ and optical fiber length L, the NSR is different in TSSB and SSB modulation. The NSR in TSSB is smaller than in SSB modulation both in single optical channel and in DWDM channels.

Chapter 3 Analysis of Nonlinear Distortion by Simulation

Nonlinear distortion in TSSB and SSB modulations were simulated by using Optsim3.6. The following simulations confirmed the theoretical analysis in Chapter 2. Parameters for all system simulation are listed in Table 3.1.

Table 3.1 System parameters.

Operating wavelength: 1550nm
Optical source: CW Laser with power 0 dBm (1mw) and linewidth FWHM 10 kHz.
Bit rate: DPSK 155Mbps.
MZM: Ideal MZM modulator with excess loss 3dB and $V_{bias} = 2.5V$, V_{π}=5V.
Linear loss of standard fiber: 0.23dB/km.
GVD of standard fiber: 16 $ps/(nm \cdot km)$.
Optical filter: Raised-Cosine.
Photo detector: PIN with quantum efficiency of 0.7, responsivity of 0.875A/W and dark current of 0.1nA.
Electrical band-pass filter: Bessel Band-pass with 3dB bandwidth 2GHz.
Electrical low-pass filter: Bessel low-pass with bandwidth 0.15GHz

3.1 Nonlinear distortion in radio over fiber system with SSB modulation and one subcarrier

One data signal with 155Mbps modulated to a 4-GHz RF carrier by DPSK modulator, and the RF signal is generated. Then this RF signal is injected to an MZM modulation system, at the optical wavelength λ =1550nm. In order to verify that the MZM modulation will generate a single sideband subcarrier and other harmonic distortions, we set the optical modulation depth $\xi\pi$ =1 and optical fiber length L=0. Then the optical spectra and eye diagram of the signal subcarrier are shown as in Figure 3.1.

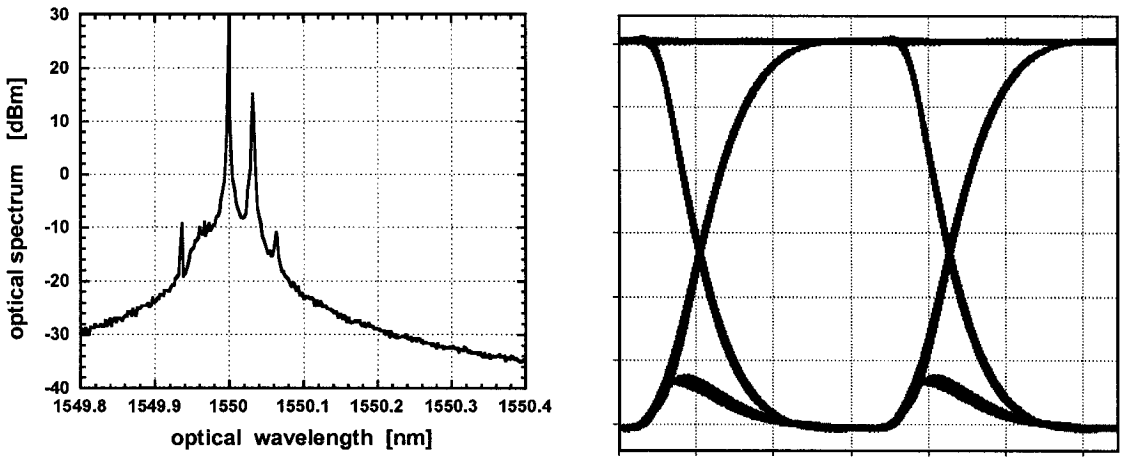

(a) (b)

Figure 3.1 (a) The optical spectra and (b) eye diagram of the single side modulation with one wavelength carry one RF signal.

From Figure 3.1(a), we got the ideal single side modulation, there is upper band subcarrier and the HDs at $\pm 2\Omega$. The other high order harmonic is too small to be shown up. And from Figure 3.1 (b), we get the very good eye diagram of this signal, because there is no nonlinear distortion with carrying only one RF subcarrier.

3.2 Nonlinear distortion in radio over fiber system with TSSB modulation and two subcarriers

In TSSB modulation, two sets of data signal with 155Mbps were modulated by DPSK electrical modulator, the radio frequencies of these two RF signals are the same with $\Omega_1 = \Omega_2 = 4$ GHz. Then the two RF signals were put into the TSSB modulation system with the optical wavelength of λ=1550nm. To be simple, we set the optical fiber length L=0. In the receiver side, we suppose that two optical filters are used to extract the optical carrier with optical signal RF1 and RF2 subcarrier respectively. After photo detection and demodulation, we got the eye diagram of the signal subcarrier. Figures 3.2, 3.3 and 3.4 show the optical spectra diagrams, and the eye diagrams of the RF signal, with the modulation depth of $\xi\pi$ = 0.1, 1, and 1.7. These two signals have the same eye diagram, and one of them is shown as example.

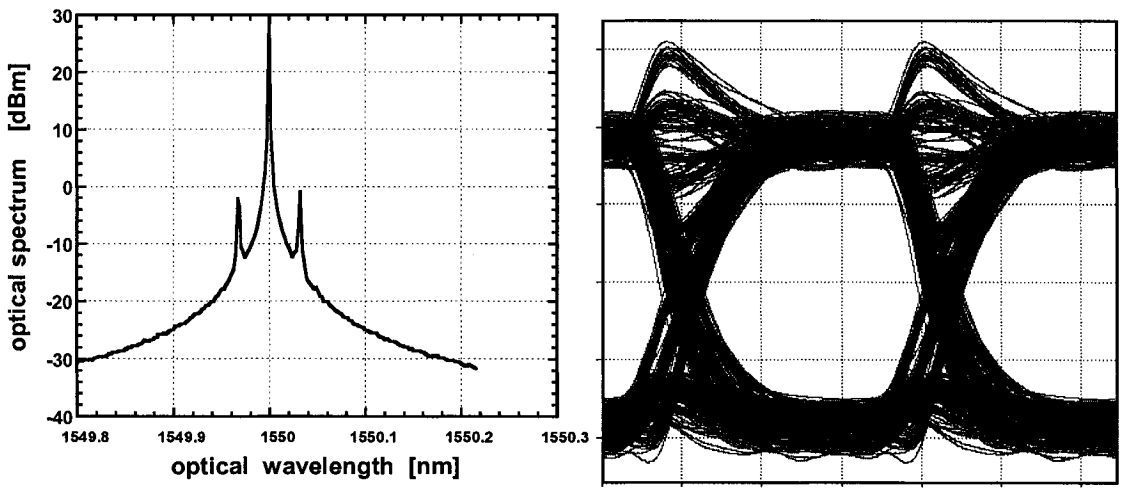

(a) (b)

Figure 3.2 (a) The optical spectra and (b) electrical eye diagram of one signal subcarrier in TSSB modulation with the modulation depth of $\xi\pi$ =0.1.

When $\xi\pi$ =0.1, the signal is very small, so the high-order harmonic at $2\Omega_1$, $2\Omega_2$ and etc are too small to be shown on the optical spectra. But the IMDs are overlapped with these two RF subcarriers, they still cause nonlinear distortion, and it is shown on the eye diagram.

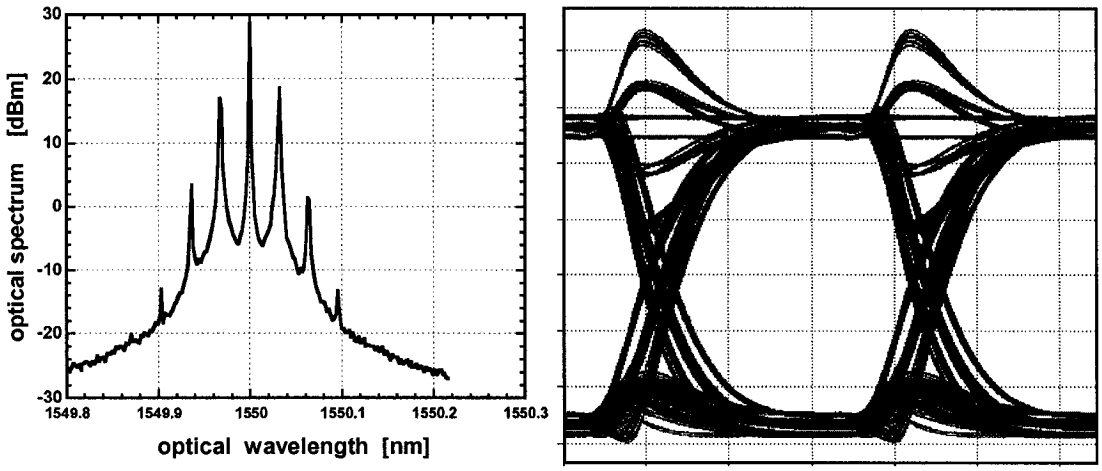

(a) (b)

Figure 3.3 (a) The optical spectra and (b) electrical eye diagram of one signal subcarrier in TSSB modulation with the modulation depth $\xi\pi$ =1.

From Figure 3.3 (a), we can see when $\xi\pi$ =1, RF1 subcarrier overlapped with IMD at $(2\Omega_1 - \Omega_2)$, and RF2 subcarrier overlapped with IMD at $(2\Omega_2 - \Omega_1)$, are increased to 18dBm. The high-order harmonic distortion at $+2\Omega_1$ and $+2\Omega_2$ overlapped and up to 2dBm, HDs at $-2\Omega_1$ and $-2\Omega_2$ overlapped and up to 3dBm, the third-order harmonics at $-3\Omega_1$ and $3\Omega_2$ are up to -5dBm. The nonlinear distortion is increased a little bit in the eye diagram, but the eye diagram is very good with eye widely opened.

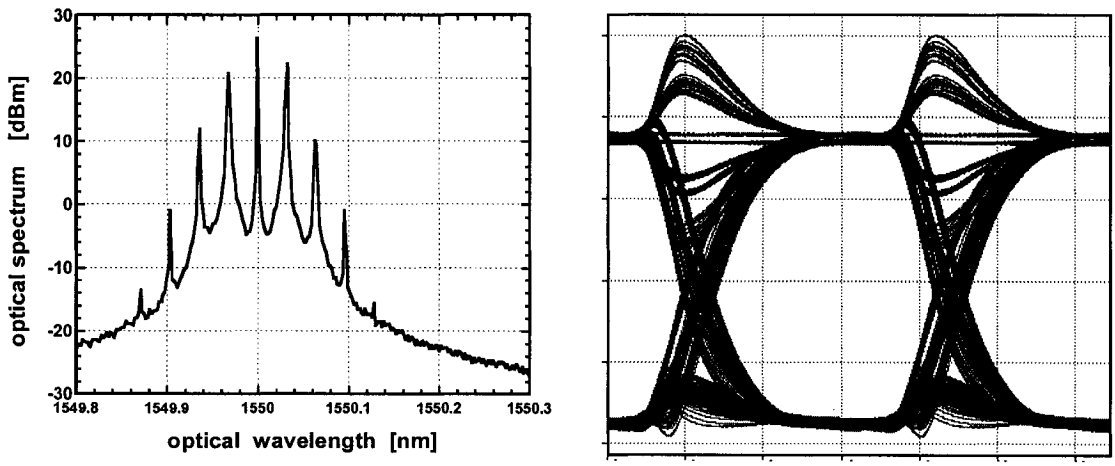

(a) (b)

Figure 3.4 (a) The optical spectra and (b) electrical eye diagram of one signal subcarrier in TSSB modulation with the modulation depth of $\xi\pi$ =1.7

From Figure 3.4 (a), we can see when $\xi\pi$ =1.7, the RF1 subcarrier overlapped with IMD at $(2\Omega_1 - \Omega_2)$, and RF2 subcarrier overlapped IMD at $(2\Omega_2 - \Omega_1)$, are increased to 22dBm. The high-order harmonic at $+2\Omega_1$ and $+2\Omega_2$ overlapped and up to 10dBm, HDs at $-2\Omega_1$ and $-2\Omega_2$ overlapped and up to 12dBm. The third-order harmonics at $-3\Omega_1$ and $3\Omega_2$ are up to 0 dBm. However the eye diagram is still very good with eye widely opened.

From the above verification, we can say that this modulation has strong anti-interference ability when the optical modulation depth is increased even to 1.7.

3.3 Nonlinear distortion in radio over fiber systems with SSB modulation and two subcarriers

In order to compare with TSSB modulation, we use the same optical wavelength as for the TSSB, the optical wavelength λ=1550nm, the frequency of the RF1 subcarrier $\Omega_1 = 4GHz$ and RF2 subcarrier $\Omega_2 = 8.5GHz$, with same data signal of 155Mbps as in TSSB, and the optical fiber length of L=0. Since these two subcarrier signals are distributed in the same sideband of the optical carrier, they got different nonlinear distortion from each other as analyzed in Section 2.3, Figure 3.5, 3.6 and 3.7 show the optical spectra diagrams and the electrical eye diagrams for RF1 and for RF2 with the modulation depth of $\xi\pi$ =0.1, 1 and 1.7.

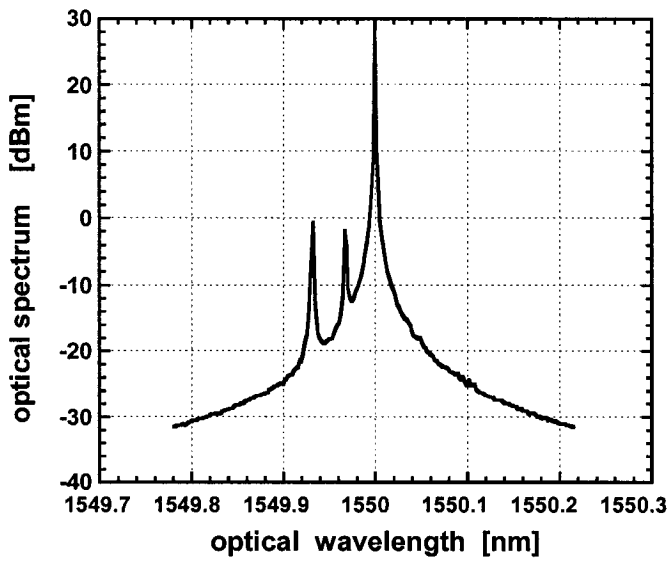

(a)

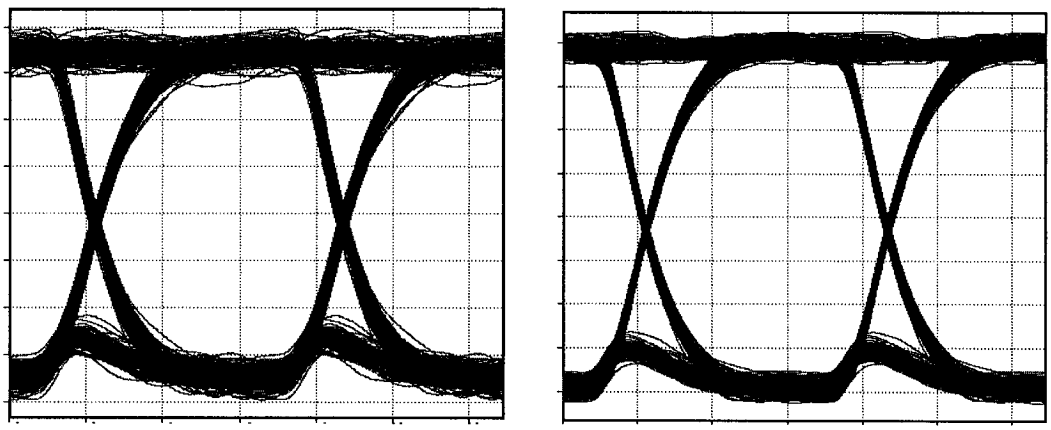

(b) (c)

Figure 3.5 (a) The optical spectra, (b) electrical eye diagrams of RF1 subcarrier and (c) eye diagram of RF2 subcarrier, with the modulation depth of $\xi\pi$ =0.1.

When $\xi\pi$ =0.1, the signal is very small, even less than 0 dBm, so the HDs and IMDs at $\pm 2\Omega_1$, $\pm(\Omega_2 - \Omega_1)$ and etc are too small to be shown on the optical spectra. Furthermore these IMD and HD are 0.5GHz away from these two subcarriers, they did not cause nonlinear distortion. So the eye diagrams are very good.

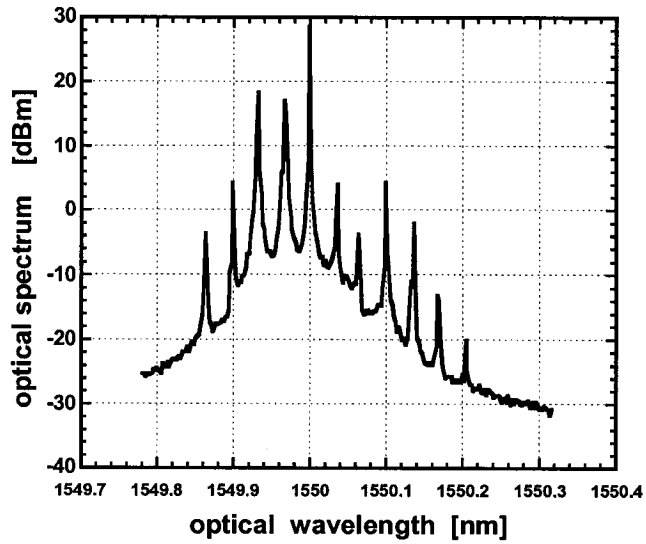

(a)

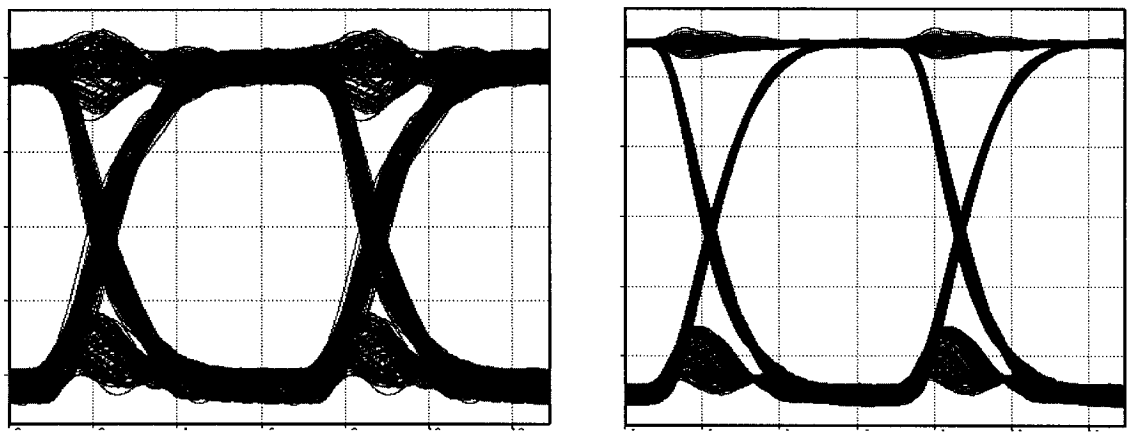

(b) (c)

Figure 3.6 (a) The optical spectra, (b) electrical eye diagrams of RF1 subcarrier and (c) eye diagram of RF2 subcarrier, with the modulation depth of $\xi\pi$ =1.

From Figure 3.6 (a), we can see when $\xi\pi$ =1, the RF1 sbucarrier is almost overlapped with IMD at $(\Omega_2 - \Omega_1)$, and RF2 subcarrier is almost overlapped with HD at $2\Omega_1$. Both subcarriers are increased to 18dBm. The IMD at $-(\Omega_2 - \Omega_1)$ is 5dBm and HD at $-2\Omega_1$ is -5dBm, and the other HDs and IMDs are also shown on the optical spectra. For the eye diagram of RF1, the nonlinear distortion is clearly shown up, and for the eye diagram of RF2, there is a small distortion.

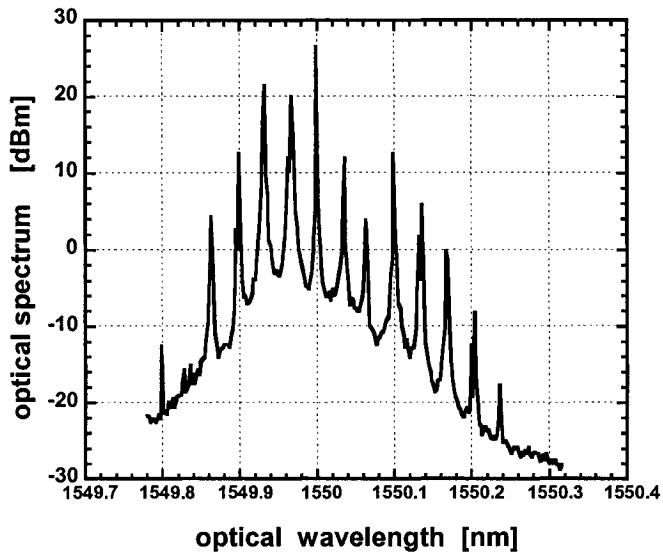

(a)

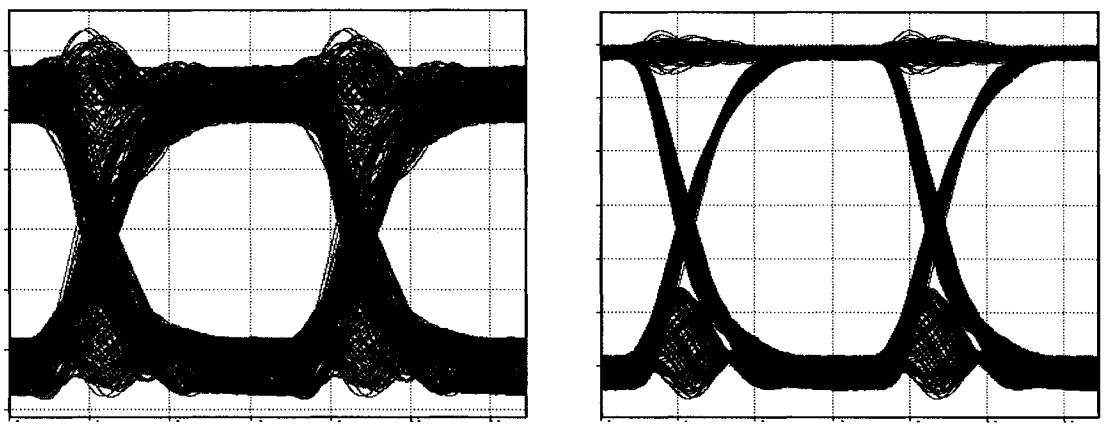

(b) (c)

Figure 3.7 (a) The optical spectra, (b) electrical eye diagrams of RF1 subcarrier and (c) eye diagram of RF2 subcarrier, with the modulation depth of $\xi\pi$ =1.7.

From Figure 3.7(a), we can see when $\xi\pi$ =1.7, the RF1 subcarrier almost overlapped with IMD at $(\Omega_2 - \Omega_1)$, and RF2 subcarrier overlapped with HD at $2\Omega_1$, are increased to 22dBm, so the IMD at $-(\Omega_2 - \Omega_1)$ is 12dBm and HD at $-2\Omega_1$ is 4dBm, and the other HDs and IMDs are also shown on the optical spectra. For the eye diagram of RF1,

the distortion is big, and for the eye diagram of RF2, there is distortion but it is not so big. The simulation verified the theoretical analysis. SSB is very good for the small signal modulations, but when the signal V_m is increased, the modulation depth is also increased, thus the nonlinear distortion will increase too. So this kind of larger modulation is not suitable for SSB modulation.

3.4 Comparison of TSSB and SSB modulations in DWDM systems

Four continual optical channels are simulated, with the optical channel space of 12.5GHz, 4 wavelengths are as follows, $\lambda_1 == 1550.1001\text{nm}$ $(\omega_1 = 193.401989032\text{THz})$ $\lambda_2 = 1550nm$ (ω_2=193.4144890THz), λ_3=1549.8998nm (ω_3=193.4269890THz), and λ_4=1549.7997nm (ω_4=193.4394890THz). We use the second optical channel for performance comparison between TSSB and SSB modulations. We also suppose that DWDM multiplexer and demultiplexer have a raised cosine optical filter with 3-dB bandwidth of 10 GHz and extinction ratio of 35dB. All the other parameters are listed in the beginning of this chapter. After demultiplexer, we still use the 12 GHz cosine-raised optical filters to get the considered optical carrier and signal subcarriers. In TSSB, we split the optical signal into two branches, then, we use the optical notch filter to remove the other subcarrier before the photo-detection. In SSB, we use the electrical filter to separate the two signal subcarriers after the photo-detector.

In TSSB modulation, we set the subcarrier frequency with $\Omega_1 = \Omega_2$ =4GHz since RF1 subcarrier is in the lower-side band and RF2 subcarrier is in the upper-side band. The IMD distortions at $-(2\Omega_1 - \Omega_2)$=-4GHz and $(2\Omega_2 - \Omega_1)$=4GHz, are overlapped with the optical signal RF1 and RF2 subcarrier, respectively. Figure 3.8 shows the simulated eye diagrams for DWDM\TSSB with $\xi\pi$ =0.1, 1.0 and 1.7 and L=25 km. From Figure3.8, we can see that the nonlinear distortion has little change with the modulation depth $\xi\pi$ is changing from 0.1, 1 to 1.7.

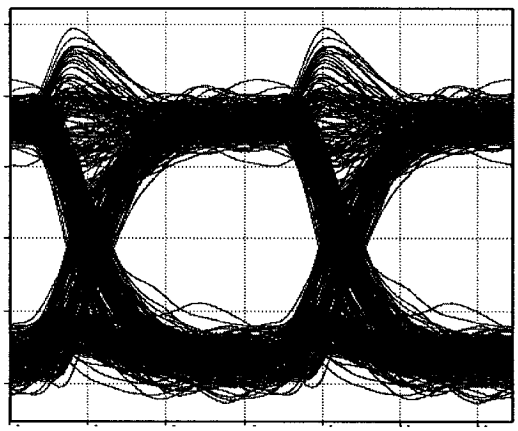

(a)

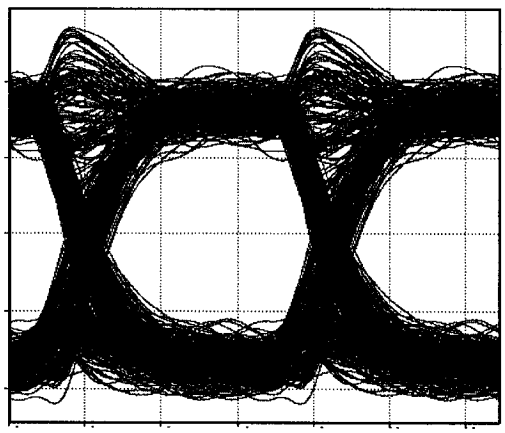

(b)

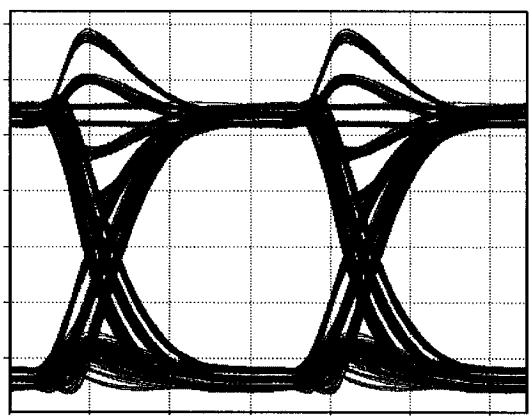

(c)

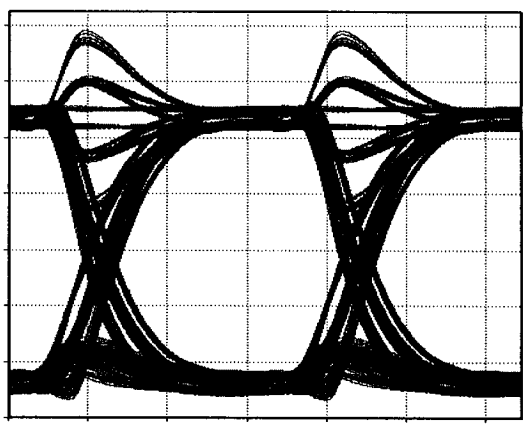

(d)

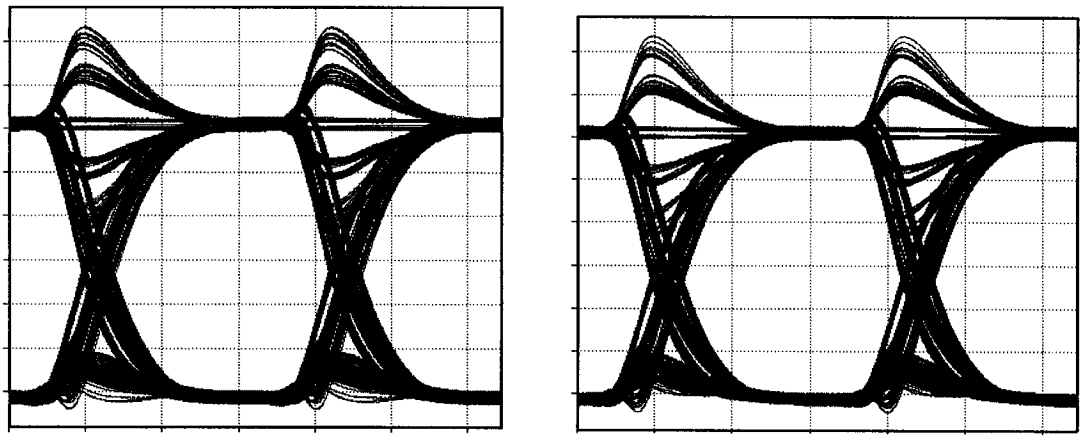

(e) (f)

Figure 3.8 The left column for eye diagram of RF signal at Ω_1 and the right column for eye diagram of RF signal at Ω_2 with modulation index of 0.1, 1.0 and 1.7.

However, in the SSB modulation we set the RF frequencies with Ω_1 =4GHz and Ω_2 =8.5GHz. Since both RF1 and RF2 subcarrier are in the same side band, so that the optical carrier and subcarrier channels will be distributed in the same as for TSSB modulation in the DWDM system.

Then we obtain Figure 3.9 which shows the eye diagrams of RF signal at Ω_1 and RF signal at Ω_2 with $\xi\pi$ =0.1, 1.0 and 1.7 and L=25Km. Compare with the Figure 3.8, for modulation depth of 1.0 and 1.7 there is bigger distortion interference in RF1 signal for SSB modulation, because HD at $2\Omega_1$ = 8GHz is 0.5GHz away from the RF2 sbucarrier and the IMD at $\Omega_2 - \Omega_1$ = 4.5GHz is 0.5GHz away from the RF1 subcarrier, and these distortions becomes big if modulation depth is big.

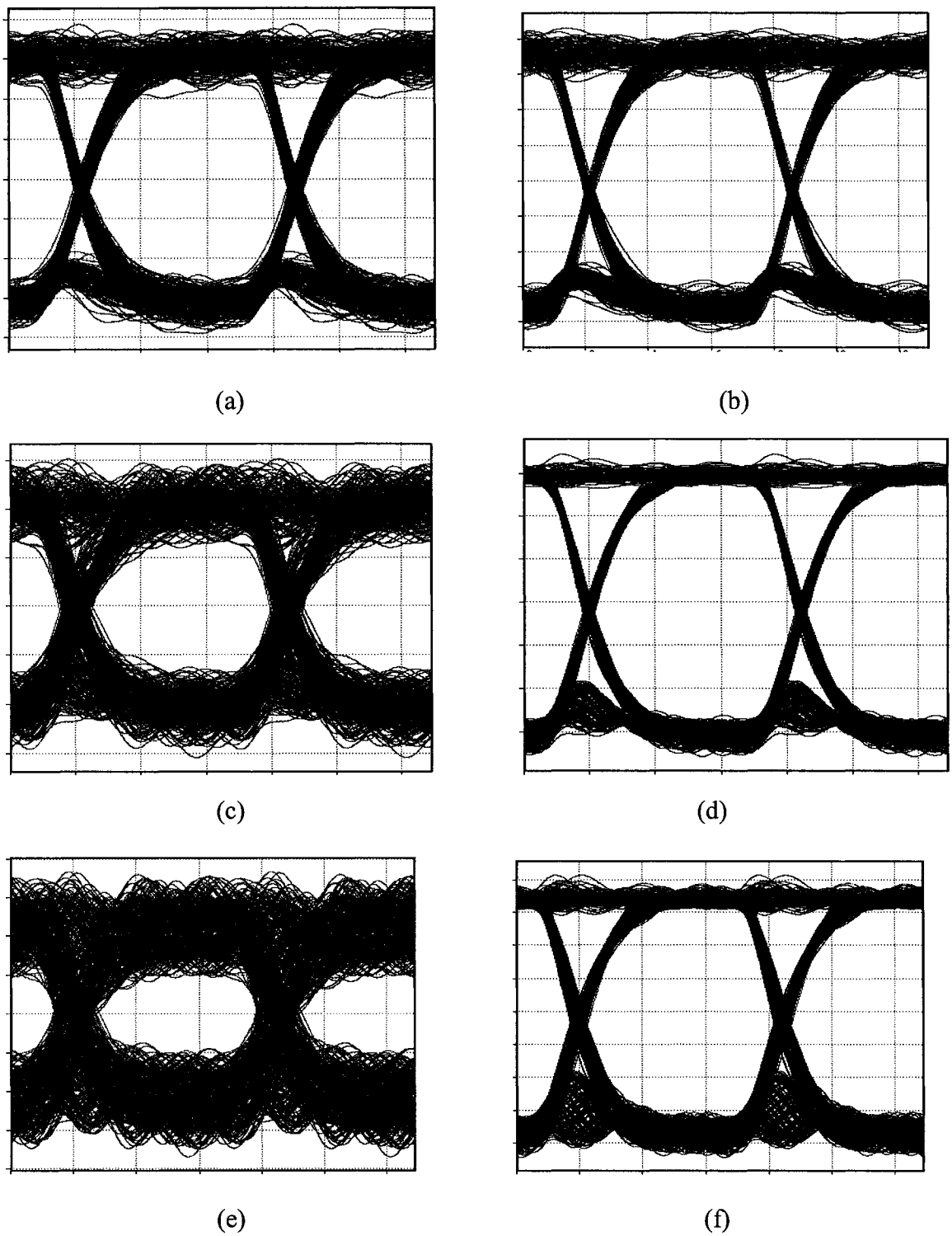

Figure 3.9 The left column for eye diagram of RF signal at Ω_1 and the right column for eye diagram of RF signal at Ω_2 with modulation index of 0.1, 1.0 and 1.7.

We further analyze the transmission performance for the DWDM with TSSB and SSB modulations by using bit error ratio vs. receiver sensitivity. We still consider the second optical channel as the example. The optical fiber of 25 km, and the modulation depths of $\xi\pi$ =0.1, 1 and 1.7 are assumed, which are shown in Figure 3.10. For small modulation depths such as $\xi\pi$ =0.1 in Figure 3.10 (a), it is observed that SSB modulation provide a better performance compared with TSSB modulation. This is because when $\xi\pi$ =0.1, the subcarrier signal is very small, the distortions are much smaller, and they are 0.5 GHz away from the subcarriers in SSB modulation, but the IMD is overlapped with the subcarrier signals in TSSB modulation. For high modulation depths such as $\xi\pi$ =1 and 1.7, see Figures 3.10 (b) and (c), it is obvious that a BER floor is induced for RF1 subcarrier of SSB modulation. This is because the distortion power of HD at $\pm 2\Omega_1$ and IMD at $\pm(\Omega_2 - \Omega_1)$ is increased much when $\xi\pi$ =1 or higher. On the other hand, TSSB modulation leads to almost independent of modulation depth in performance. This is because the power of IMDs at $(2\Omega_1 - \Omega_2)$ and $-(2\Omega_2 - \Omega_1)$ is increased almost the same as the subcarriers when $\xi\pi$ =1 or higher.

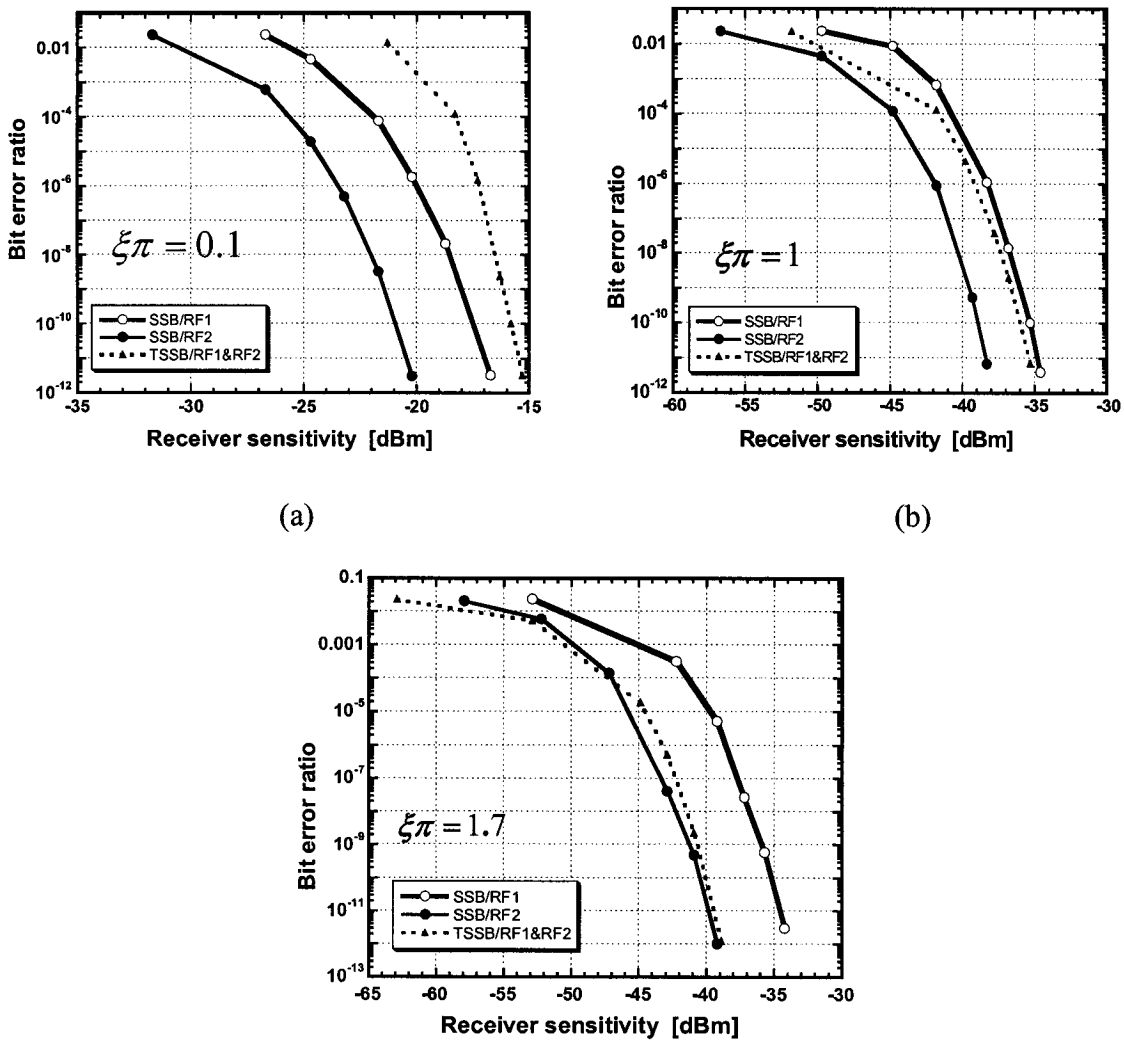

Figure 3.10 The receiver sensitivity in TSSB and SSB with the optical cable is 25km, the modulation depth is (a) $\xi\pi$ =0.1, (b) $\xi\pi$ =1 and (c) $\xi\pi$ =1.7 respectively.

3.5 Summary

All the nonlinear distortion analyzed theoretically in Chapter 2 is verified by simulations. From the optical spectra diagrams, simulations show that nonlinear distortion exists in optical subcarrier modulations, and the nonlinear distortion HDs and IMDs are increased when the optical modulation depth $\xi\pi$ is increased from 0.1 to 1 and to 1.7 in TSSB and SSB modulations. In TSSB modulation, the signal eye diagrams do not change much even when the HDs and IMDs are largely increased, however in SSB modulation, the eye diagram of RF1 become worse obviously when the optical modulation depth $\xi\pi$ is changed from 0.1 to 1.7. In the DWDM application, for optical modulation depth of $\xi\pi$ =0.1, SSB modulation has better eye diagram than TSSB. With small optical modulation depth of $\xi\pi$ =0.1, SSB modulation provides a better performance compared with TSSB modulation. However when $\xi\pi$ =1 or higher, TSSB modulation is shown better anti-interference ability and better receiver sensitivity performance.

Chapter 4 Conclusion

We have theoretically investigated nonlinear distortion induced by optical subcarrier modulation. The two popular subcarrier modulations, i.e. TSSB and SSB, were considered and compared in the generation of nonlinear distortion, consisting of inter-modulation distortion and harmonic distortion between the RF subcarriers in the same optical channel. The distortion mostly depends on the optical modulation depth $\xi\pi$ in both TSSB and SSB modulations. In TSSB modulation, NSRs for RF1 and RF2 are also depend on the subcarrier frequency and optical fiber length. However in SSB modulation, NSR for RF2 subcarrier mainly depends on the optical modulation depth $\xi\pi$, and the frequency Ω_2. but NSR for RF1 subcarrier depends on not only the optical modulation depth $\xi\pi$ and the frequency Ω_1, but also the optical fiber length L. In the same modulation depth $\xi\pi$, RF frequency and optic fiber length L, NSR in TSSB is smaller than that in SSB modulation in single RoF systems.

Besides the interference from the same optical channel, in the DWDM system there is nonlinear distortion from the neighbor optical channels both in TSSB and SSB modulations. In order to compare the TSSB with SSB modulation in DWDM application,

we set the $\Omega_1=\Omega_2$=4GHz in TSSB and Ω_1=4GHz, Ω_2=8.5GHz in SSB, so that the optical channels will be distributed evenly and the same in both DWDM systems. Then, NSR in TSSB and SSB modulation is very small when the optical modulation depth of $\xi\pi$=0.1, and the nonlinear distortion can be ignored. However when $\xi\pi$=1 or higher, the NSR of RF1 or RF2 in TSSB is 5 to10dB less than the NSR in SSB modulation. We also analyzed the relationship between the receiver sensitivity and the bit error ratio in DWDM systems with the same optical wavelengths, RF frequency, fiber length and optical modulation depth $\xi\pi$. When $\xi\pi$=0.1, both subcarriers in SSB modulation has better performance than in TSSB modulation. However when $\xi\pi$=1 or 1.7, the performance in TSSB is becoming better, the performance of RF1 in SSB modulation become worse. So SSB modulation is suitable to small optical modulation depth ($\xi\pi$=0.1), and TSSB modulation is suitable to normal or big optical modulation depth ($\xi\pi$=1 to 1.7).

$$\cos(x\sin\theta) = J_0(x) + 2\sum_{n=1}^{\infty} J_{2v}(x)\cos 2n\theta$$

$$\sin(x\sin\theta) = 2\sum_{n=1}^{\infty} J_{2v-1}(x)\sin(2n-1)\theta$$

we got the followings,

$$E = \frac{E_0}{\sqrt{2}}\left\{\cos\omega t\left[-2\sum_{n=1}^{\infty} J_{2n-1}(\xi\pi)\sin(2n-1)\left(\Omega_1 t + \frac{\pi}{2}\right)\times\left(J_0(\xi\pi) + 2\sum_{n=1}^{\infty} J_{2n}(\xi\pi)\cos 2n\Omega_2 t\right)\right.\right.$$

$$-2\sum_{n=1}^{\infty} J_{2n-1}(\xi\pi)\sin(2n-1)\Omega_2 t\times\left(J_0(\xi\pi) + 2\sum_{n=1}^{\infty} J_{2n}(\xi\pi)\cos 2n\left(\Omega_1 t + \frac{\pi}{2}\right)\right)$$

$$+\left(J_0(\xi\pi) + 2\sum_{n=1}^{\infty} J_{2n}(\xi\pi)\cos 2n\Omega_1 t\right)\times\left(J_0(\xi\pi) + 2\sum_{n=1}^{\infty} J_{2n}(\xi\pi)\cos 2n\left(\Omega_2 t + \frac{\pi}{2}\right)\right)$$

$$\left.-2\sum_{n=1}^{\infty} J_{2n-1}(\xi\pi)\sin(2n-1)\Omega_1 t\times 2\sum_{n=1}^{\infty} J_{2n-1}(\xi\pi)\sin(2n-1)\left(\Omega_2 t + \frac{\pi}{2}\right)\right]$$

$$-\sin\omega t\left[\left(J_0(\xi\pi) + 2\sum_{n=1}^{\infty} J_{2n}(\xi\pi)\cos 2n\left(\Omega_1 t + \frac{\pi}{2}\right)\right)\times\left(J_0(\xi\pi) + 2\sum_{n=1}^{\infty} J_{2n}(\xi\pi)\cos 2n\Omega_2 t\right)\right.$$

$$-2\sum_{n=1}^{\infty} J_{2n-1}\sin(2n-1)\left(\Omega_1 t + \frac{\pi}{2}\right)\times 2\sum_{n=1}^{\infty} J_{2n-1}\sin(2n-1)\Omega_2 t$$

$$+2\sum_{n=1}^{\infty} J_{2n-1}(\xi\pi)\sin(2n-1)\Omega_1 t\times\left(J_0(\xi\pi) + 2\sum_{n=1}^{\infty} J_{2n}(\xi\pi)\cos 2n\left(\Omega_2 t + \frac{\pi}{2}\right)\right)$$

$$\left.\left.+2\sum_{n=1}^{\infty} J_{2n}(\xi\pi)\sin 2n\Omega_1 t\times 2\sum_{n=1}^{\infty} J_{2n-1}(\xi\pi)\sin(2n-1)\left(\Omega_2 t + \frac{\pi}{2}\right)\right]\right\}$$

After simplification we get

$$E_{out} = \frac{E_0}{\sqrt{2}}\left\{\sqrt{2}J_0{}^2(\xi\pi)\cos\left(\omega t + \frac{\pi}{4}\right) - 2J_0(\xi\pi)J_1(\xi\pi)\cos(\omega t + \Omega_1 t) - 2J_0(\xi\pi)J_1(\xi\pi)\sin(\omega t - \Omega_2 t)\right.$$

$$\left.+\sqrt{2}J_1{}^2(\xi\pi)\sin\left(\omega t + (\Omega_2 - \Omega_1)t - \frac{\pi}{4}\right) - \sqrt{2}J_1{}^2(\xi\pi)\sin\left(\omega t - (\Omega_2 - \Omega_1)t - \frac{\pi}{4}\right)\right.$$

$$+\sqrt{2}J_1^{\,2}(\xi\pi)\sin\left(\omega t+(\Omega_2+\Omega_1)t+\frac{\pi}{4}\right)-\sqrt{2}J_1^{\,2}(k)\sin\left(\omega t-(\Omega_1+\Omega_2)t+\frac{\pi}{4}\right)$$

$$-2J_1(\xi\pi)J_2(\xi\pi)\cos\left(\omega t-(2\Omega_2+\Omega_1)t\right)+2J_1(\xi\pi)J_2(\xi\pi)\cos\left(\omega t-(2\Omega_2-\Omega_1)t\right)$$

$$+2J_1(\xi\pi)J_2(\xi\pi)\sin(\omega t+(2\Omega_1+\Omega_2)t)+2J_1(\xi\pi)J_2(\xi\pi)\sin(\omega t+(2\Omega_1-\Omega_2)t)$$

$$+\sqrt{2}J_0(\xi\pi)J_2(\xi\pi)\cos\left(\omega t+2\Omega_1 t-\frac{\pi}{4}\right)+\sqrt{2}J_0(\xi\pi)J_2(\xi\pi)\cos\left(\omega t-2\Omega_1 t-\frac{\pi}{4}\right)$$

$$-\sqrt{2}J_0(\xi\pi)J_2(\xi\pi)\cos\left(\omega t+2\Omega_2 t-\frac{\pi}{4}\right)-\sqrt{2}J_0(\xi\pi)J_2(\xi\pi)\cos\left(\omega t-2\Omega_2 t-\frac{\pi}{4}\right)$$

$$-2J_2^2(\xi\pi)\cos\left(\omega t+2(\Omega_2-\Omega_1)t+\frac{\pi}{4}\right)-2J_2^2(\xi\pi)\cos\left(\omega t-2(\Omega_2-\Omega_1)t+\frac{\pi}{4}\right)$$

$$+2J_0(\xi\pi)J_3(\xi\pi)\cos(\omega t-3\Omega_1 t)+2J_0(\xi\pi)J_3(\xi\pi)\sin(\omega t+3\Omega_2 t)+\cdots\}$$

2. SSB

From the MZM modulator, we got the modulated optical signal as follows,

$$E=\frac{E_0}{\sqrt{2}}\left\{\cos\omega t\left(\cos\left(\frac{\pi}{2}+\xi\pi\cos\Omega_1 t+\xi\pi\cos\Omega_2 t\right)+\cos(\xi\pi\sin\Omega_1 t+\xi\pi\sin\Omega_2 t)\right)\right.$$

$$\left.-\sin\omega t\left(\sin\left(\frac{\pi}{2}+\xi\pi\cos\Omega_1 t+\xi\pi\cos\Omega_2 t\right)+\sin(\xi\pi\sin\Omega_1 t+\xi\pi\sin\Omega_2 t)\right)\right\}$$

$$E=\frac{E_0}{\sqrt{2}}\{\cos\omega t(-\sin(\xi\pi\cos\Omega_1 t+\xi\pi\cos\Omega_2 t)+\cos(\xi\pi\sin\Omega_1 t+\xi\pi\sin\Omega_2 t))$$

$$-\sin\omega t(\cos(\xi\pi\cos\Omega_1 t+\xi\pi\cos\Omega_2 t)+\sin(\xi\pi\sin\Omega_1 t+\xi\pi\sin\Omega_2 t))\}$$

$$E=\frac{E_0}{\sqrt{2}}\{\cos\omega t[-\sin(\xi\pi\cos\Omega_1 t)\cos(\xi\pi\cos\Omega_2 t)-\cos(\xi\pi\cos\Omega_1 t)\sin(\xi\pi\cos\Omega_2 t)$$

$$+\cos(\xi\pi\sin\Omega_1 t)\cos(\xi\pi\sin\Omega_2 t)-\sin(\xi\pi\sin\Omega_1 t)\sin(\xi\pi\sin\Omega_2 t)]$$

$$-\sin\omega t[\cos(\xi\pi\cos\Omega_1 t)\cos(\xi\pi\cos\Omega_2 t)-\sin(\xi\pi\cos\Omega_1 t)\sin(\xi\pi\cos\Omega_2 t)$$

APPENDIX

Detailed mathematic derivation of the electrical field output from an MZM modulator in TSSB and SSB modulations.

1. TSSB

From the MZM modulator, we got the modulated optical signal as follows,

$$E = \frac{E_0}{\sqrt{2}}\left\{\cos\omega t\left(\cos\left(\frac{\pi}{2} + \xi\pi\cos\Omega_1 t + \xi\pi\sin\Omega_2 t\right) + \cos\left(\xi\pi\sin\Omega_1 t + \xi\pi\cos\Omega_2 t\right)\right)\right.$$
$$\left. - \sin\omega t\left(\sin\left(\frac{\pi}{2} + \xi\pi\cos\Omega_1 t + \xi\pi\sin\Omega_2 t\right) + \sin\left(\xi\pi\sin\Omega_1 t + \xi\pi\cos\Omega_2 t\right)\right)\right\}$$

$$E = \frac{E_0}{\sqrt{2}}\{\cos\omega t\left(-\sin\left(\xi\pi\cos\Omega_1 t + \xi\pi\sin\Omega_2 t\right) + \cos\left(\xi\pi\sin\Omega_1 t + \xi\pi\cos\Omega_2 t\right)\right)$$
$$- \sin\omega t\left(\cos\left(\xi\pi\cos\Omega_1 t + \xi\pi\sin\Omega_2 t\right) + \sin\left(\xi\pi\sin\Omega_1 t + \xi\pi\cos\Omega_2 t\right)\right)\}$$

$$E = \frac{E_0}{\sqrt{2}}\{\cos\omega t[-\sin\left(\xi\pi\cos\Omega_1 t\right)\cos\left(\xi\pi\sin\Omega_2 t\right) - \cos\left(\xi\pi\cos\Omega_1 t\right)\sin\left(\xi\pi\sin\Omega_2 t\right)$$
$$+ \cos\left(\xi\pi\sin\Omega_1 t\right)\cos\left(\xi\pi con\Omega_2 t\right) + \cos\left(\xi\pi\sin\Omega_1 t\right)\sin\left(\xi\pi\cos\Omega_2 t\right)]$$
$$- \sin\omega t[\cos\left(\xi\pi\cos\Omega_1 t\right)\cos\left(\xi\pi\sin\Omega_2 t\right) - \sin\left(\xi\pi\cos\Omega_1 t\right)\sin\left(\xi\pi\sin\Omega_2 t\right)$$
$$+ \sin\left(\xi\pi\sin\Omega_1 t\right)\cos\left(\xi\pi\cos\Omega_2 t\right) + \cos\left(\xi\pi\sin\Omega_1 t\right)\sin\left(\xi\pi\cos\Omega_2 t\right)]\}$$

After we use the Bessel function,

$$+\sin(\xi\pi\sin\Omega_1 t)\cos(\xi\pi\sin\Omega_2 t)+\cos(\xi\pi\sin\Omega_1 t)\sin(\xi\pi\sin\Omega_2 t)]\}$$

We still use the Bessel function, and we got the modulated optical signal,

$$E=\frac{E_0}{\sqrt{2}}\left\{\cos\omega t\left[-2\sum_{n=1}^{\infty}J_{2n-1}(\xi\pi)\sin(2n-1)\left(\Omega_1 t+\frac{\pi}{2}\right)\times\left(J_0(\xi\pi)+2\sum_{n=1}^{\infty}J_{2n}(\xi\pi)\cos 2n\left(\Omega_2 t+\frac{\pi}{2}\right)\right)\right.\right.$$

$$-2\sum_{n=1}^{\infty}J_{2n-1}(\xi\pi)\sin(2n-1)\left(\Omega_2 t+\frac{\pi}{2}\right)\times\left(J_0(\xi\pi)+2\sum_{n=1}^{\infty}J_{2n}(\xi\pi)\cos 2n\left(\Omega_1 t+\frac{\pi}{2}\right)\right)$$

$$+\left(J_0(\xi\pi)+2\sum_{n=1}^{\infty}J_{2n}(\xi\pi)\cos 2n\Omega_1 t\right)\times\left(J_0(\xi\pi)+2\sum_{n=1}^{\infty}J_{2n}(\xi\pi)\cos 2n\Omega_2 t\right)$$

$$\left.-2\sum_{n=1}^{\infty}J_{2n-1}(\xi\pi)\sin(2n-1)\Omega_1 t\times 2\sum_{n=1}^{\infty}J_{2n-1}(\xi\pi)\sin(2n-1)\Omega_2 t\right]$$

$$-\sin\omega t\left[\left(J_0(\xi\pi)+2\sum_{n=1}^{\infty}J_{2n}(\xi\pi)\cos 2n\left(\Omega_1 t+\frac{\pi}{2}\right)\right)\times\left(J_0(\xi\pi)+2\sum_{n=1}^{\infty}J_{2n}(\xi\pi)\cos 2n\left(\Omega_2 t+\frac{\pi}{2}\right)\right)\right.$$

$$-2\sum_{n=1}^{\infty}J_{2n-1}(\xi\pi)\sin(2n-1)\left(\Omega_1 t+\frac{\pi}{2}\right)\times 2\sum_{n=1}^{\infty}J_{2n-1}(\xi\pi)\sin(2n-1)\left(\Omega_2 t+\frac{\pi}{2}\right)$$

$$+2\sum_{n=1}^{\infty}J_{2n-1}(\xi\pi)\sin(2n-1)\Omega_1 t\times\left(J_0(\xi\pi)+2\sum_{n=1}^{\infty}J_{2n}(\xi\pi)\cos 2n\Omega_2 t\right)$$

$$\left.\left.+\left(J_0(\xi\pi)+2\sum_{n=1}^{\infty}J_{2n}(\xi\pi)\cos 2n\Omega_1 t\right)\times 2\sum_{n=1}^{\infty}J_{2n-1}(\xi\pi)\sin(2n-1)\Omega_2 t\right]\right\}$$

After simplification, we get

$$E_{out}=\frac{E_0}{\sqrt{2}}\left\{\sqrt{2}J_0{}^2(\xi\pi)\cos\left(\omega t+\frac{\pi}{4}\right)\right.$$

$$-2J_0(\xi\pi)J_1(\xi\pi)\cos(\omega t+\Omega_1 t)-2J_0(\xi\pi)J_1(\xi\pi)\cos(\omega t+\Omega_2 t)$$

$$\left.-\sqrt{2}J_1{}^2(\xi\pi)\cos\left(\omega t+(\Omega_2+\Omega_1)t+\frac{\pi}{4}\right)-\sqrt{2}J_1{}^2(k)\cos\left(\omega t-(\Omega_1+\Omega_2)t+\frac{\pi}{4}\right)\right.$$

$$+\sqrt{2}J_1^{\,2}(\xi\pi)\cos\left(\omega t+(\Omega_2-\Omega_1)t-\frac{\pi}{4}\right)+\sqrt{2}J_1^{\,2}(\xi\pi)\cos\left(\omega t-(\Omega_2-\Omega_1)t-\frac{\pi}{4}\right)$$

$$+\sqrt{2}J_0(\xi\pi)J_2(\xi\pi)\cos\left(\omega t+2\Omega_1 t-\frac{\pi}{4}\right)+\sqrt{2}J_0(\xi\pi)J_2(\xi\pi)\cos\left(\omega t-2\Omega_1 t-\frac{\pi}{4}\right)$$

$$+\sqrt{2}J_0(\xi\pi)J_2(\xi\pi)\cos\left(\omega t+2\Omega_2 t-\frac{\pi}{4}\right)+\sqrt{2}J_0(\xi\pi)J_2(\xi\pi)\cos\left(\omega t-2\Omega_2 t-\frac{\pi}{4}\right)$$

$$+2J_1(\xi\pi)J_2(\xi\pi)\cos(\omega t-(2\Omega_2+\Omega_1)t)+2J_1(\xi\pi)J_2(\xi\pi)\cos(\omega t+(2\Omega_2-\Omega_1)t)$$

$$+2J_1(\xi\pi)J_2(\xi\pi)\cos(\omega t-(2\Omega_1+\Omega_2)t)+2J_1(\xi\pi)J_2(\xi\pi)\cos(\omega t+(2\Omega_1-\Omega_2)t)$$

$$+2J_2^2(\xi\pi)\cos\left(\omega t+2(\Omega_2-\Omega_1)t+\frac{\pi}{4}\right)+2J_2^2(\xi\pi)\cos\left(\omega t-2(\Omega_2-\Omega_1)t+\frac{\pi}{4}\right)$$

$$+2J_0(\xi\pi)J_3(\xi\pi)\cos(\omega t-3\Omega_1 t)+2J_0(\xi\pi)J_3(\xi\pi)\cos(\omega t-3\Omega_2 t)+\cdots\Big\}$$

References

[1] H Ogawa, D Polifko and S Banba, "Millieter-wave fiber optical systems for personal radio communication," *IEEE Trans. on Microwave Theory and Technique*, vol. 40, No. 12, pp.2294-2302, Dec. 1992.

[2] D. Wake, D. Johansson and D. Moodie, "Passive picocell: a new concept in wireless network infrastructure," *Electron. Lett.*, vol.33, pp.404-406, Feb. 1997.

[3] J. Yu, J. Gu, X. Liu, Z. Jia, and G. Chang, "Seamless integration of an 8x2.5 Gb/s WDM PON and radio over fiber using all-optical up-conversion based on Raman assisted FWM," *IEEE Photonics Technol. Lett.*, vol.17, pp.1986-1988, Sept. 2005.

[4] T. Ismail, C. Liu, J. Mitchell, A. Seeds, X. Qian, A. Wonfor, R. Penty, and I. White, "Transmission of 37.6-GHz QPSK wireless data over 12.8-km fiber with remote millimeter wave local oscillator delivery using a bidirectional SOA in a full-duplex system with 2.2-km CWDM fiber ring architecture," *IEEE Photonics Technol. Lett.*, vol.17, pp.1989-1991, Sept. 2005.

[5] W. Chen and W. Way, "Multi-channel signal-sideband SCM/DWDM transmission systems," *J. Lightwave Technol.*, vol.22, pp.1679-1693, July 2004.

[6] R. Hui, "Multi-tributary OFDM optical transmitter using carrier-suppressed optical

single-sideband modulation," in *Proceeding of Optical Fiber Communications Conference 2003*, pp. 92-93.

[7] M. Bakaul, A. Nirmalathas, and C. Lim, "Multi-functional WDM optical interface for millimeter wave fiber-radio Antenna base station," *J. Lightwave Technol.,* vol.23, pp.1210-1218, Mar. 2005.

[8] C. Lim, A. Nirmalathas, M. Attygalle, D. Novek, and R. Waterhouse, "On the merging of milliter-wave fiber-radio backbone with 25 GHz WDM ring networks," *J. Lightwave Technol.,* vol.21, pp.2203-2210, Oct. 2003.

[9] H. Toda, T. Yamashita, T. Kuri, and K. Kitayama, "Demultiplexing using an arrayed-waveguide grating for frequency interleaved DWDM millimeter-wave radio on fiber systems," *J. Lightwave Technol.,* vol.21, pp.1735-1741, Aug. 2003.

[10] T. Kuri, and K. Kitayama, "Optical heterodyne detection techniques for densely multiplexed millimeter-wave band radio on fiber systems," *J. Lightwave Technol.*, vol.21, pp.3167-3179, 2003.

[11] G. Smith, D. Novak and Z. Ahmed, "Technique for optical SSB generation to overcome dispersion penalties in fiber-radio system," *Electron. Lett.,* vol.33, pp. 74-75, Jan. 1997.

[12] G. Smith, D. Novak and Z. Ahmed, "Overcoming chromatic dispersion effects in fiber-wireless systems incorporating external modulators," *IEEE Tran. Microwave Theory and Techniques,* vol.45, pp.1410-1415, Aug. 1997.

[13] A. Narasimha, X. Meng, M. Wu, and E. Yablonovitch, "Tandem single-side band

modulation scheme for doubling spectral efficiency of analogue fiber links," *Electron. Lett.,* vol.36, pp.1135-1136, Jun. 2000.

[14] P. Laurencio and M. Medeiros, "Dynamic range of optical links employing optical single side-band modulation," *IEEE Photonics Technol. Lett.*, vol.15, pp.748-750, May 2003.

[15] H. Lu, S. Tzeng, and Y. Liu, "Intermodulation distortion suppression in a full-duplex radio over fiber ring networks," *IEEE Photonics Technol. Lett.*, vol.16, pp.602-604, Feb. 2004.

[16] L. Roselli, V. Borgioni, F. Zepparelli, F. Ambrosi, M. Comez, P. Faccin, and A. Casini, "Analog laser pre-distortion for multi-service radio over fiber systems," *J. Lightwave Technol.*, vol.21, pp.1211-1223, May 2003.

[17] H. Schmuck, "Comparison of optical millimeter-wave system concepts with regard to chromatic dispersion," *Electron. Lett.,* vol.31, pp.1848-1849, Oct. 1995.

[18] F. Ramos and J. Marti, "Frequency transfer function of dispersive and nonlinear single-mode optical fibers in microwave optical systems," *IEEE Photonics Technol. Lett.*, vol.12, pp. 549-551, May 2000.

[19] M. Phillips and D. Ott, "Crosstalk due to optical fiber nonlinearities in WDM CATV lightwave systems," *J. Lightwave Technol.*, vol.17, pp.1782-1792, Oct. 1999.

[20] T. Kuri and K. Kitayama, "Optical heterodyne detection technique for densely multiplexed millimeter-wave –band radio-on-fiber systems," *J. Lightwave Technol.,* vol.21, pp.3167-3178, Dec. 2003.

[21] M. Phillips and D. Ott, "Crosstalk caused by non-ideal output filters in WDM light wave systems," *IEEE Photonics Technol. Lett.,* vol.12, pp. 1094-1096, Aug. 2000.

[22] A. Cartaxo, B. Wedding, and W. Idler, "Influence of fiber nonlinearity on the fiber transfer function: theoretical and experimental analysis," *J. Lightwave Technol.,* vol.17, pp.1806-1813, Oct. 1999.

[23] R. Hui, B. Zhu, R. Huang, C. Allen, K. Demarest, and D. Richards, "Subcarrier multiplexing for high-speed optical transmission," *J. Lightwave Technol.,* vol.20, pp.417-427, Mar. 2002.